A PRINTED CIRCUIT BOARD FOR THE MEASUREMENT OF MULTIPLE BIOLOGICAL VITAL SIGNALS USING BIOIMPEDANCE TECHNIQUES

A Thesis

by

GILBERTO OSMAR FLORES REYES

Submitted to the Graduate and Professional School of
Texas A&M University
in partial fulfillment of the requirements for the degree of

MASTER OF SCIENCE

Chair of Committee,	Gerard L. Coté
Committee Members,	Jean-Francois Chamberland
	Raffaella Righetti
	Saurabh Biswas
Head of Department,	Aniruddha Datta

August 2022

Major Subject: Electrical Engineering

ABSTRACT

The noninvasive measurement of vital signs, particularly for cardiovascular and respiratory disease, is of great importance, since it can be used for monitoring the progress of a patient's condition. In fact, monitoring the progress of a patient after they have left the hospital can be just as important as while they are in the hospital. For this reason, many companies as well as research institutions are developing wearable devices that can continuously monitor the vital signs of a patient. A common way to measure vital signs such as heart rate and respiration rate is by using light-based methods, but they have some weaknesses such as relatively high energy consumption. Hence, it is important to continue to develop alternative sensing systems.

The goal of this research is to develop a small form factor bioimpedance circuit that captures artery pulsation, which can then be used to obtain vital signs such as heart rate and respiration rate. Bioimpedance itself is an electrical-based sensing method which consists of injecting a small current and then measuring the voltage change. The developed bioimpedance circuit consists of three sections: (1) a section to generate a high single-frequency, low current signal to be injected into the body, (2) a section to capture and measure the voltage differential generated across two points in the subject's body due to the current injected, and (3) a section that takes the measured voltage differential and processes it to obtain the desired bioimpedance signal. From the bioimpedance signal, one can then obtain physiologically relevant information such as heart rate, and respiration rate.

DEDICATION

Dedico éste trabajo a mi Familia, porque siempre me han apoyado y es gracias a ellos que tengo la oportunidad de desarrollarme como persona y como ingeniero.

ACKNOWLEDGEMENTS

I would like to thank my committee chair, Dr. Coté, and my committee members, Dr. Biswas, Dr. Righetti, and Dr. Chamberland for being on my committee.

Thanks also go to my friends and colleagues and the department faculty and staff for making my time at Texas A&M University a great experience.

Finally, I would like to thank my family for their continuous support.

CONTRIBUTORS AND FUNDING SOURCES

Contributors

This work was supervised by a thesis committee consisting of Professor Gerard L. Coté (chair), Professor Saurabh Biswas of the Department of Biomedical Engineering, and Professor Raffaella Righetti, Professor Jean-Francois Chamberland of the Department of Electrical and Computer Engineering.

All work conducted for the thesis was completed by the student, under the advisement of Professor Gerard L. Coté of the Department of Biomedical Engineering.

Funding Sources

This work was made possible in part by [funding source] under Grant Number [insert grant number]. Its contents are solely the responsibility of the authors and do not necessarily represent the official views of the [name of awarding office].

TABLE OF CONTENTS

Page

LIST OF FIGURES

LIST OF TABLES

1. INTRODUCTION

1.1 Cardiovascular and respiratory disease

The number one cause of death on a global level is cardiovascular disease. Just in 2019 alone, the number of people that died from cardiovascular disease was 18.56 million. The third cause of death are respiratory diseases and in the same year, 3.97 million people around the world died [1]. Looking for example in the United States, one person will die every 36 seconds from cardiovascular disease. This means that in total, around 660,000 people will die from this cause, representing 25% of all deaths in the US [2]. In fact, as a general trend, the main cause of death greatly depends on the country's income. In lower income countries, infectious diseases are the main cause of death and in higher income countries, non-communicable diseases, such as cardiovascular disease, dominate as the main cause of death [2].

Looking at projections for 2030, it is expected that 40.5 percent of the total population in the US will have cardiovascular disease. This will represent 800 billion (billion in short scale) USD in potential costs [3]. However, there is one big issue that many people and organizations overlook whenever talking about these types of noncommunicable diseases in diverse countries such as the US. This is, the fact that these diseases impact disproportionately underserved communities, such as African Americans. African Americans have higher risk of developing hypertension and diabetes which in turn, also increase the risk of developing and/or increase the severity of cardiovascular disease [4]. In fact, in 2009, it was measured that 0.387% of African American males and 0.2679% of African American females died from cardiovascular disease, whereas the average in the US was 0.2361% of the population that died from cardiovascular disease [4]. Hispanic

populations are also at a disadvantage, where cardiovascular disease represents their number one cause of death.

1.2 Tracking cardiovascular and respiratory disease

For people that have noncommunicable diseases such as cardiovascular and respiratory disease, tracking their condition is a key part of the process for them to recover. This is essential to determine whether a person's condition is getting better or worse so that then, the physician is able to act accordingly.

All health workers, from physicians to paramedics, utilize mainly four vital signs to noninvasively monitor the patient's condition: heart rate, respiration rate, blood pressure, and body temperature [5]. Since tracking the patient's condition is of great importance, hospitals are equipped with expensive and robust devices designed to measure the vital signs while the patients are in the hospital. However, the same cannot always be said for when after a patient leaves the hospital. For this very reason, many institutions are on a race trying to develop wearable devices that can track physiological vital signs such as heart rate and respiration rate.

Several different methods exist for obtaining physiological signals using wearable devices such as: electrocardiography, photoplethysmography, and bioimpedance, for example. The most common method used in most commercial, fitness wearable devices in the market is photoplethysmography [6]. This light-based method is more popular because it is simple to setup and operate, can be incorporated into a simple form factor like a watch device, and is relatively inexpensive while still being reasonably effective as a fitness device [7].

There are already commercial, wearable devices that are advertised as fitness trackers such as the Fitbit, Garmin smartwatch and the Apple Watch [6]. The intent is that such devices can be used to help people monitor their fitness and exercise to ultimately promote a change to a healthier lifestyle [6] [8]. Looking specifically at the Apple Watch, it has been cleared by the Food and Drug Administration as a Class II device for "Electrocardiograph software for over-the-counter use" and data generated is not intended for clinical use or to diagnose or treat a person [9]. A Class II device refers to those that present moderate to high risk to the user. Hence, further development is needed to create wearable devices that can help track accurately vital signs, which can then be useful for tracking cardiovascular and respiratory disease.

1.3 Disparity in wearable devices

It is worth noting that, not only do African Americans and Hispanic Americans have more predisposition to develop and die from cardiovascular disease, many of the tracking devices just mentioned are not made taking into account the inherent biological differences that these populations have. So even when they are supposed to be made to measure important physiological vital signs such as heart rate and respiratory rate, they might not work as effectively for different populations.

As an example, one can look at most wrist-worn watches in the market today. Studies have been performed that show that when people with darker skin tone use photoplethysmography-based wearable sensors, the chosen wavelength for the device is not as effective for their skin color so there is a decrease in the accuracy of quality of the signals obtained [10]. This is because, depending on the wavelength used in the device, it will influence how deep light signal can reach into the tissue for different skin tones.

High Body Mass Index is also a factor that is highly present in these communities, and which has been proven to significantly impact the waveform of signals captured using photoplethysmography [11]. The reason for the decrease in signal quality is because higher BMI levels represents more tissue layers for the light to go through, and thus, the shape of the obtained waveform will be impacted.

It is for these reasons that it is necessary to develop wearable devices which can accomplish their function for everyone, taking into account the overlooked segments of the population just mentioned. One potential solution that can be implemented is to use bioimpedance techniques to measure the vital signs. In this way, one can take a first step towards creating a wearable sensor for more diverse populations. The reasoning for this is that bioimpedance measures the same artery pulsation as photoplethysmography, but since biological tissue has different electrical and optical properties, the penetration into the tissue with bioimpedance is deeper and the waveform is potentially less susceptible to changes due to skin tone.

2. BACKGROUND

2.1 Impedance spectroscopy and motivation

Impedance Spectroscopy measurement techniques have existed for many years and can be used in a great variety of fields such as the oil industry, electrochemistry, bioimpedance and other applications [12,13,14]. At a basic level, the way in which it works is that, by the application of some current or voltage into the object of interest, one can then obtain information about the object in the form of the resulting impedance. This is done by measuring the voltage or current generated across that object. With this information, one can then determine characteristics of the measured system and/or how the system changes with time [15].

Bioimpedance itself, is a form of impedance spectroscopy, where it is applied to the human body. There are plenty of applications already in place which prove bioimpedance itself is a working and valid method to use. For example, bioimpedance is already used in many commercial scales, where they send a harmless current through the body and in doing so, they can obtain information about the bone density, water, and fat content in the person's body and even can be used to measure body cell mass [16]. Another application of bioimpedance is to be able to detect cardiac and respiratory activity in a non-invasive manner. For example, this technique has been proven to obtain important cardiac activity information in the radial artery located in the wrist, as well as respiratory activity information obtained by measuring motion from the thorax [17].

A great location in the body where one can apply bioimpedance techniques is on the brachial artery in the upper arm. The reasoning is that it is easier to obtain respiratory activity information in this location since, every time a person inhales and exhales, the

upper arm can move along with the chest and this motion can be captured by bioimpedance. At the same time, measuring in the brachial artery still allows us to obtain cardiac activity information as it would in any other artery. However, there have not been many attempts to apply the bioimpedance technique on the brachial artery in the upper arm, and the ones that have, did not capture both heart and respiratory activity in the data they produced [18,19]. This opens up the possibility for the development of a system which is capable of measuring in the upper arm both cardiac and respiratory activity simultaneously.

2.2 Bioimpedance method

For the reasons mentioned in the previous subsection, the interest of this research is to utilize bioimpedance to obtain both cardiac and respiratory activity from artery/arteriole pulsation and arm motion respectively, in a non-invasive manner. As stated before, a simple explanation of how bioimpedance works is that a signal is injected into the body, and then the generated signal is measured from the body. To start developing a system, the first thing that needs to be done is to understand what signal is injected into the body and the rationale behind it.

In general, one can inject a single frequency or multiple frequencies into tissue, and depending on the value of the frequency chosen, it will provide different information about the object. One can classify the frequencies into three ranges based on the dispersion they have on human tissue: α-dispersion (Hz-kHz), β-dispersion (kHz-MHz) and γ-dispersion at higher frequencies. In general, the β-dispersion range is more informative for the application we are interested in since it provides information about the cell membranes and

whole blood [20]. For this reason, a frequency in the β-dispersion range is chosen as the frequency of injection for our application.

After the frequency is chosen, one needs to determine whether the applied signal will be voltage or current-based and also, what amplitude it will have. In terms of regulations and standards, according to the IEC 60601-1-11, the root mean square current of the signal injected into the body depends on the frequency. Since regulations are based on limiting how much current one can inject, most bioimpedance systems are current-injecting, instead of voltage-injecting. When selecting a current amplitude, it will be upper-limited depending on what frequency the signal injected contains [21]. It follows the following formula:

$$I_{rms} \leq 10^{-7} f$$

where I_{rms} units are Amperes and f units are Hz.

Once a specific frequency has been chosen, the upper-limit for the current rms amplitude is known. Now, after injecting the chosen current into the body, the next step is to capture the generated voltage differential across two points. To do this, one needs to understand how information about the artery pulsation is captured after injecting a current into the body. The way it works is that every time an artery pulsates, its effective impedance value changes. If we measure this impedance change over a period of time, one can capture the full artery pulsation waveform, after appropriate signal processing. This waveform can then be used to obtain the previously mentioned physiological parameters.

To capture this, a high precision instrumentation amplifier is necessary so it can capture the voltage differential while adding little noise to the signal. The signal then needs to be acquired with an Analog to Digital Converter (ADC) with high enough bit resolution

and sampling rate. Additionally, to extract the signal of interest from the captured voltage by the ADC, signal processing needs to be performed. It can either be done in the computer in post-processing or using analog components before acquiring it with the ADC.

3. DESIGN, DEVELOP AND TEST OF BIOIMPEDANCE CIRCUIT

3.1 Approach

Before developing the full circuit, and as a first step to be taken for this research, the minimum necessary circuit sections needed to obtain bioimpedance signal will be developed. These are the current injection section as well as the signal measuring section. By having only, the necessary sections of the circuit, one can determine if they are functioning correctly. To visualize the resulting signal, processing can be done in the computer at this stage. The system will be evaluated first based on correct functionality and capability of obtaining bioimpedance signal.

3.2 Literature search on bioimpedance-based sensing

To be able to develop a bioimpedance sensing circuit, different papers were read that explain the physiology behind it, as well as the acquisition process, and the potential components required for it to work correctly. First, reading was done to understand the physiology behind bioimpedance. In general, bioimpedance is part of the more general category of Impedance Plethysmography, which means that changes in volume in the body are measured indirectly from changes in electrical impedance [22]. For us, to measure the strongest artery pulsation waveform, it is necessary to inject and measure the signal directly on top of the artery with the electrodes running parallel to it.

Once potential locations for injection and measurement are known, one should decide how many electrodes to use. In general, there are two methods for injecting and measuring the signal. The first method consists of using two electrodes that both inject and measure the signal simultaneously. This method is less preferred due to the fact that this configuration adds unwanted resistance which comes from the electrode tissue interface

and it will affect the final measurement [23,24]. One could argue that this additional impedance could be characterized to then be eliminated from the measurement. However, this resistance is not constant as a function of time because the electrode tissue interface can change due to physiological processes such as perspiration or pathological ones such as fibrosis or necrosis.

The second method consists of using four electrodes. The most common four electrode configuration, known as the Wenner or Schlumberger arrangement, has the two most outer electrodes inject the current and the two inner electrodes measure the resulting voltage [25]. The reason for this being the preferred method is that this configuration eliminates the electrode tissue interface impedance and other unknown contact impedances as well. [24, 26, 27]. Another reason why the four electrode configuration is preferred for our application is that, at the frequency range chosen for this project (~ kHz), the four electrode method adds really small impedance to the measurement, whereas the two method electrode adds greater impedance [28].

In Figure 1, one can observe how signal will be applied and measured using the four electrode method. The external electrodes are used for injecting the current and it can be observed that one side is the positive terminal and the other is the negative terminal. Then, the inner electrodes are used for measuring the voltage differential generated across the tissue. The figure illustrates how to apply the current on top of the artery, and how the impedance change is due to the variation of its cross-sectional area caused by change in blood flow. Furthermore, since the blood flow change in the artery is directly caused by heart beating, the impedance variation $\triangle Z(t)$ is directly related to heart rate.

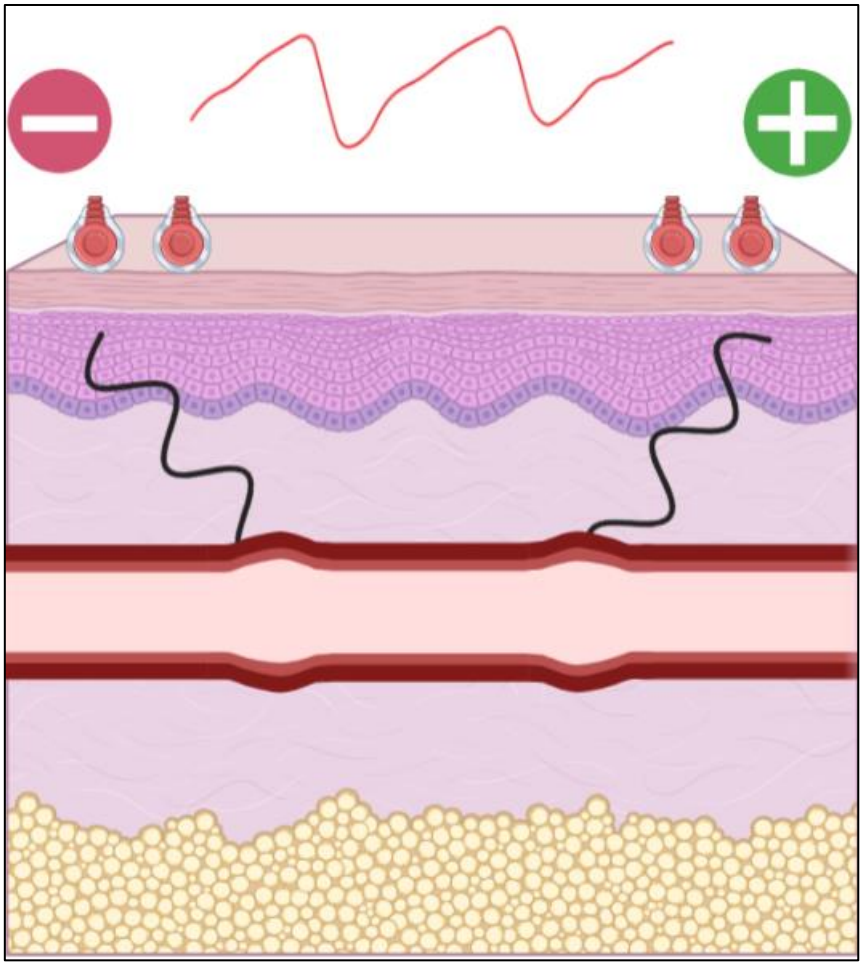

Figure 3.1 – Illustration of current injection for bioimpedance acquisition

3.3 Component selection and test circuit

3.3.1 Signal generator for Injection section

The injection section of the circuit can be divided into two main subsections: the signal generator and the voltage to current converter. The purpose of the signal generator subsection is to make a periodic signal with a single frequency. The frequency will be chosen in the β-dispersion range as mentioned previously, that is, in the kilohertz range. One can choose to use a Digital to Analog Converter chip to generate the signal or build an oscillator analog circuit. Both of them achieve the same function so the oscillator analog

circuit was chosen for its simplicity and scalability in case one wanted to mass produce the created system.

At a basic level, oscillator circuits require an amplifier and appropriate feedback. The selected operational amplifier must have low noise, high common mode rejection and open loop gain. For this reason, to make the analog oscillator circuit, high precision operational amplifiers are used since it is required for the frequency to be exact. For our application, the OPA277 high precision chip was chosen since it meets our requirements as it can be observed in Table 3.1 [29].

Table 3.1: Electrical characteristics for OPAx277P

Parameter	**Typical Value**	**Unit**
Input Voltage Noise Density	8	nV/√Hz
Common Mode Rejection	80	dB
Open loop gain	40	dB

One can make oscillators using either inductors and capacitors (LC) configurations or resistors and capacitors (RC) configurations. For the kilohertz frequency range required for this application, RC configurations are preferred. The reason is that, to generate frequencies that are relatively low, the inductance values needed are non-practically high for LC oscillators. The chosen analog oscillator circuit configuration is known as Wien Bridge Oscillator.

The Wien Bridge Oscillator is composed of parallel and series RC components, connected to an amplifier, which has appropriate resistors connected to it for gain as it can be observed in Figure 3.2 [30].

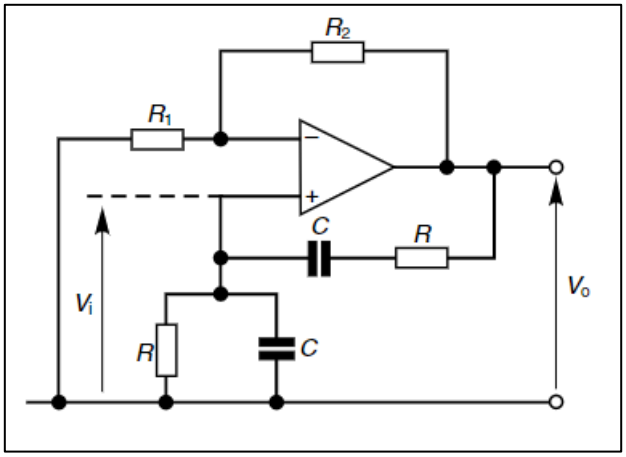

Figure 3.2. Wein Bridge Oscillator circuit configuration

By analyzing the circuit, one can obtain the ratio of the voltage input Vin and the voltage output Vout as follows:

$$\frac{V_{in}}{V_{out}} = \frac{R||\frac{1}{j\omega C}}{R||\frac{1}{j\omega C} + R + \frac{1}{j\omega C}} = \frac{1}{3 + j\left(\omega RC - \frac{1}{\omega RC}\right)}$$

It is known that at the frequency of oscillation of the circuit, the phase shift must be zero. To do this, one can set the imaginary part equal to zero to eliminate any phase components. In doing so, the following equation must be true:

$$\omega RC - \frac{1}{\omega RC} = 0 \rightarrow \omega RC = \frac{1}{\omega RC}$$

It is observed that one obtains a quadratic equation in ω as a function of R and C. Since it is a quadratic equation, there are two potential solutions, and one might obtain negative solutions, but they will be discarded since negative solutions do not make

physical sense. To determine what ω is as a function of R and C, we need to solve the previous equation:

$$\omega^2 = \frac{1}{(RC)^2} \rightarrow \omega = \pm\frac{1}{RC} \rightarrow \omega = \frac{1}{RC}$$

Now, one can select the frequency of oscillation for the Wein Bridge circuit by selecting desired values for R and C. The values for R and C were selected taking two things into consideration: (1) the desired kilohertz frequency range of oscillation, and (2) the standard values available for resistors and capacitors, trying to choose the most common ones. After calculating different combinations, the chosen values are: R = 1800 Ω and C = 4.7 nF. Choosing these values, one obtains:

$$\omega = 2\pi f \rightarrow f = \frac{1}{2\pi RC} = \frac{1}{2\pi(1800)(4.7x10^{-9})} \cong 19\ kHz$$

Going back to the ratio of Vin and Vout, whenever $\omega = \frac{1}{RC}$, there is an attenuation of 1/3 which must be compensated by making the amplifier have a gain of at least 3 V/V:

$$\text{Attenuation: } \frac{V_{in}}{V_{out}} = \frac{1}{3+j\left(\left(\frac{1}{RC}\right)RC - \frac{1}{\left(\frac{1}{RC}\right)RC}\right)} = \frac{1}{3+j(1-1)} = \frac{1}{3}$$

$$\text{Gain: } \frac{V_{out}}{V_{in}} = 1 + \frac{R_2}{R_1} \geq 3 \rightarrow \frac{R_2}{R_1} \geq 2$$

For this, standard, common values are chosen with $R_2 = 100\ k\Omega$ and $R_1 = 47\ k\Omega$.

3.3.2 Voltage to current converter for Injection section

Now that we can produce an oscillating voltage using the Wien Bridge, we have to convert it to a current signal using a voltage to current converter. The function of the voltage to current converter subsection is to take as input the voltage generated in the oscillator subsection, and output it as a low and stable current value. The voltage to current

converter is done by using an Improved Howland Current Pump configuration which can be observed in Figure 3.3 [31].

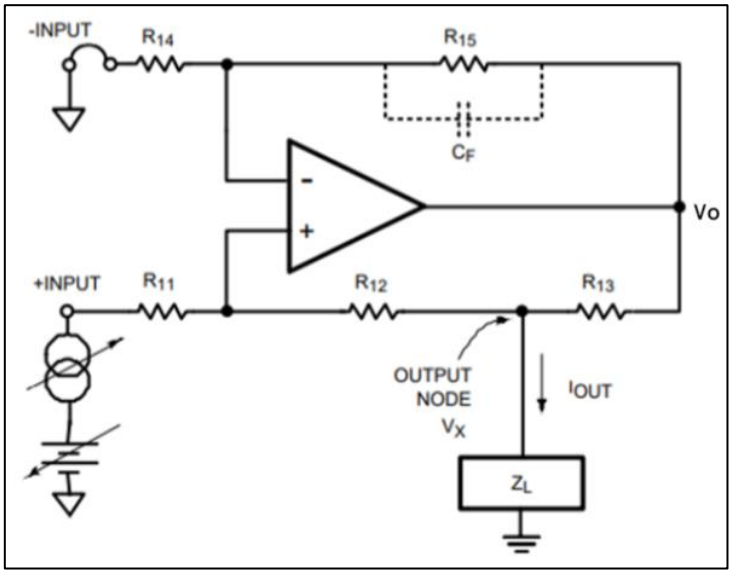

Figure 3.3. Improved Howland Current Pump configuration

Again, we utilize an OPA277 as the amplifier for this subsection. The values chosen for the different resistors will determine the rms amplitude of the current signal, which as we know, is upper-limited depending on the frequency of oscillation chosen in the previous subsection. By doing node analysis of this configuration one can obtain:

$$I_{OUT} = \frac{V_{in+} - V_x}{R_{11} + R_{12}} + \frac{V_o - V_x}{R_{13}}$$

$$V_o = \left(1 + \frac{R_{15}}{R_{14}}\right)\left(V_x + R_{12}\frac{V_{in+} - V_x}{R_{11} + R_{12}}\right) = \frac{(R_{15} + R_{14})(V_x R_{11} + R_{12}V_{in+})}{R_{14}(R_{11} + R_{12})}$$

Using the previous two equations, one can obtain I_{OUT} as a function of V_{in+} and V_x:

$$I_{OUT} = \frac{V_{in+} - V_x}{R_{11} + R_{12}} + \frac{(R_{15} + R_{14})(V_x R_{11} + R_{12}V_{in+})}{R_{13}R_{14}(R_{11} + R_{12})} - \frac{V_x}{R_{13}}$$

$$I_{OUT} = V_{in+}\left[\frac{1}{R_{11} + R_{12}} + \frac{R_{12}(R_{15} + R_{14})}{R_{13}R_{14}(R_{11} + R_{12})}\right] + V_x\left[\frac{R_{11}(R_{15} + R_{14})}{R_{13}R_{14}(R_{11} + R_{12})} - \frac{1}{R_{13}} - \frac{1}{R_{11} + R_{12}}\right]$$

Since we want to make I_{OUT} independent of V_x (the voltage generated across the tissue), we need to make its coefficient equal to zero:

$$\frac{R_{11}(R_{15}+R_{14})}{R_{13}R_{14}(R_{11}+R_{12})}-\frac{1}{R_{13}}-\frac{1}{R_{11}+R_{12}}=\frac{R_{11}(R_{15}+R_{14})-R_{14}(R_{11}+R_{12})-R_{13}R_{14}}{R_{13}R_{14}(R_{11}+R_{12})}=0$$

$$\frac{R_{11}R_{15}-R_{14}(R_{12}+R_{13})}{R_{13}R_{14}(R_{11}+R_{12})}=0$$

After simplifying the coefficient of V_x and setting it equal to zero, the expression will be zero whenever the numerator is equal to zero:

$$R_{11}R_{15}-R_{14}(R_{12}+R_{13})=0\rightarrow R_{11}R_{15}=R_{14}(R_{12}+R_{13})\rightarrow R_{11}=R_{14},R_{15}=R_{12}+R_{13}$$

By choosing the resistors values as described, one can assure that the output current of the Howland Current pump will be independent of the load connected to it. Then, the output current depends only on the following:

$$I_{OUT}=V_{in+}\left[\frac{1}{R_{11}+R_{12}}+\frac{R_{12}(R_{12}+R_{13}+R_{11})}{R_{13}R_{11}(R_{11}+R_{12})}\right]=V_{in+}\left[\frac{1}{R_{11}+R_{12}}+\frac{R_{12}^2+R_{12}R_{13}+R_{12}R_{11}}{R_{13}R_{11}^2+R_{13}R_{11}R_{12}}\right]$$

In general, R_{14} is chosen to be equal to R_{15} so $R_{11}=R_{12}+R_{13}$, then:

$$I_{OUT}=V_{in+}\left[\frac{1}{2R_{12}+R_{13}}+\frac{2R_{12}(R_{12}+R_{13})}{R_{13}(R_{12}+R_{13})^2+R_{13}R_{12}(R_{12}+R_{13})}\right]=V_{in+}\left[\frac{1}{2R_{12}+R_{13}}+\frac{2R_{12}}{R_{13}^2+2R_{13}R_{12}}\right]$$

$$I_{OUT}=V_{in+}\left[\frac{2R_{12}+R_{13}}{R_{13}(2R_{12}+R_{13})}\right]=\frac{V_{in+}}{R_{13}}$$

Now, in an elegant simplification, the current is a function of only V_{in+} and R_{13}. This means that if we want to increase the amplitude of the current, we have to either increase the amplitude of the input voltage or decrease the resistance of R_{13}. Now the values for all resistors can be chosen and generally, R_{13} can be kept at a low resistance such as 2.7 kΩ and be modified depending on the desired output current, and all other resistors can be chosen to have high resistance such as 100 kΩ.

3.3.3 Measurement section

After selecting what configurations to use and values for the injection section of the circuit, one can go ahead and select what component to use for measuring the resulting voltage across the person's tissue. Making this part of the circuit is simpler since the only thing needed is an instrumentation amplifier which has low noise and high common mode rejection ratio. At this stage, the measuring will be done by using an INA828 since it covers our requirements as seen in Table 3.2 [32]:

Table 3.2: Electrical characteristics for INA828

Parameter	Typical Value (for G = 10)	Unit
Input Voltage Noise Density	12	nV/√Hz
Common Mode Rejection	100	dB

The gain is set by a resistor and it depends the given formula: $G = 1 + \frac{50\ k\Omega}{R_G}$ [31]. To achieve a gain of ~10, one should select R_G to be ~ $5\ k\Omega$. Since the bioimpedance signal that we are interested in is really small, the ADC needs to have a high number of bits. Additionally, since the signal that we have to acquire contains a ~19 kHz frequency, the sampling rate needs to be at a minimum twice that frequency. For these reasons, the output of the measuring section from the INA828 is acquired with a NI-DAQmx acquisition device, which contains 16 bits in the ADC and is capable of reaching up to 500 kSamples/s, which for our application will be 100 kHz [33]. This signal will then go into a computer where it will be processed. Now, the circuit can be built and tested according to Figure 3.4.

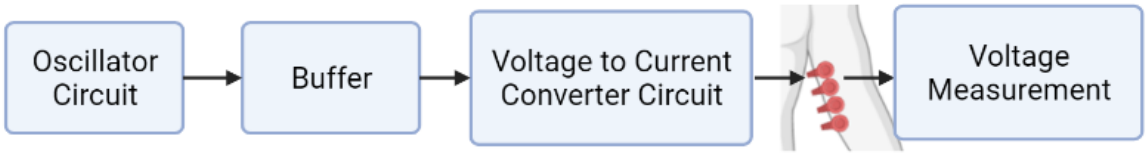

Figure 3.4 Flow diagram of bioimpedance circuit

3.3.4 Test circuit

To assess the design, a test subject will utilize the research-grade bioimpedance machine, Biopac MP160 with the EBI100C attachment. to obtain bioimpedance signal [34, 35]. Then, the same subject will obtain bioimpedance signal from the developed circuit. The obtained bioimpedance signal from the developed circuit and the Biopac machine will be compared in morphology to each other to ensure the waveform shapes are similar to each other and that one can go ahead build a printed circuit board to reduce any potential noise. This experiment was carried out by connecting the electrodes in the selected Wenner configuration and placed on top of the artery. In Figures 3.5 and 3.6 one can observe the results from the Biopac system and the developed circuit. One can also showcase the 1st derivative of the bioimpedance signal to better visualize the peaks from the bioimpedance signal.

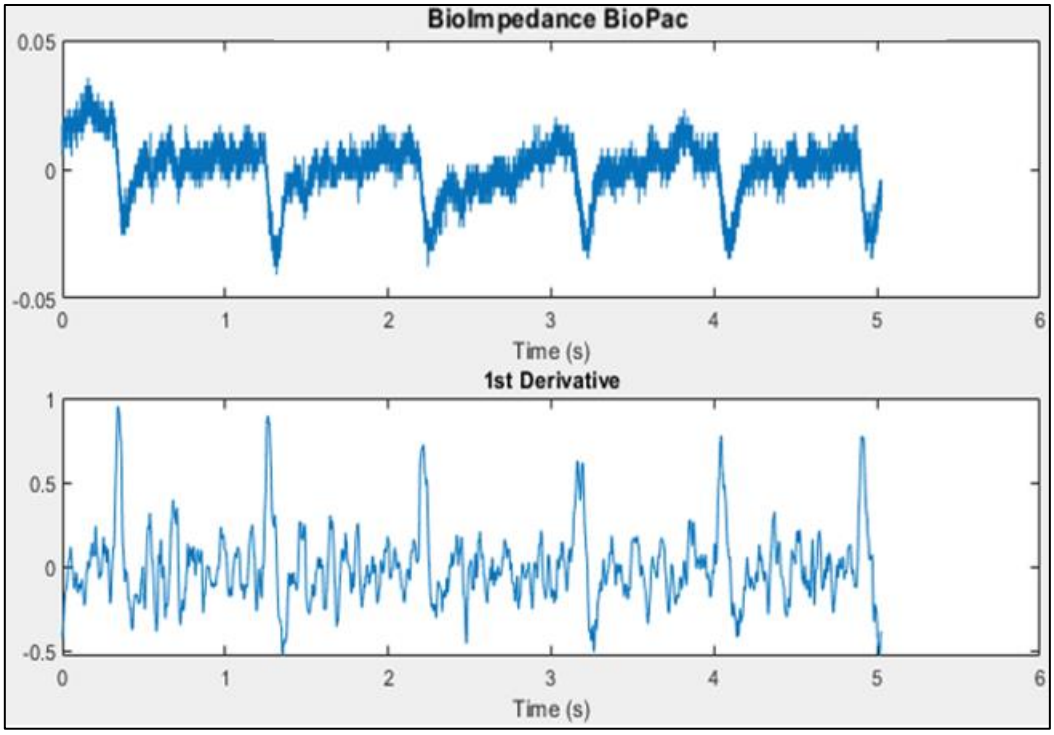

Figure 3.5 Bioimpedance signal obtained with Biopac

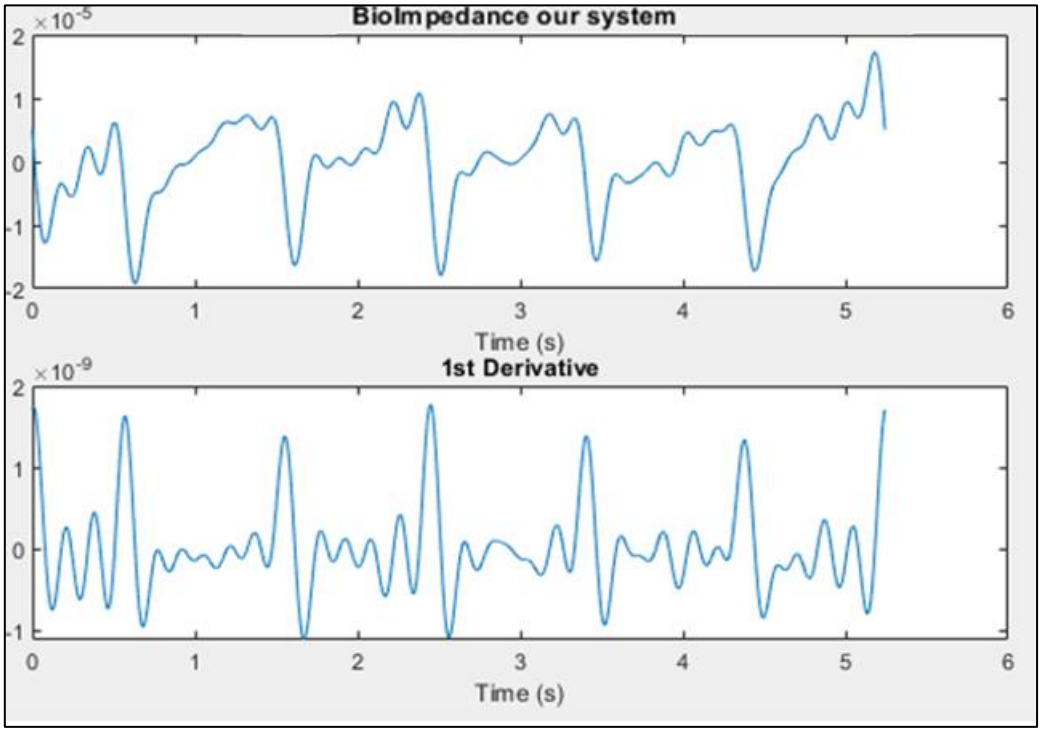

Figure 3.6 Bioimpedance signal obtained with circuit

In Figure 3.5, the data obtained from the Biopac machine is presented. It has a built-in 10 Hz lowpass filter, although it can be seen that it still has great amounts of noise. In Figure 3.6, the data obtained from the circuit is presented. Signal processing was done in MATLAB to extract the desired bioimpedance signal, as well as a 6 Hz lowpass filter. One can observe that the obtained signal from both systems are similar in morphology, so one can go ahead and build the printed circuit board version of the system. This, ideally, will be beneficial in terms of noise, since there are less moving parts from the components in the breadboard.

3.4 Develop schematic, printed circuit board and test circuit

3.4.1 Develop schematic

The first step to develop the bioimpedance printed circuit board using the Altium software, is to develop a schematic. This is done since the software uses the components and their connections in the schematic to create connections for the 3D printed circuit board. In Figure 3.7 and Figure 3.8, one can observe the developed schematic to generate the bioimpedance circuit.

As mentioned, the Oscillator circuit is generating a voltage signal with a 19 kHz frequency and 3.13 V/V gain. The buffer is placed in between the two section to avoid any loading of the oscillator circuit. The Voltage to Current Converter circuit takes in the voltage signal, and outputs it as a current signal, which can then be injected into the person. Finally, the measurement section consists of the INA828 instrumentation amplifier with a gain of 10 V/V. Some capacitors are added to remove any DC offset there might exist.

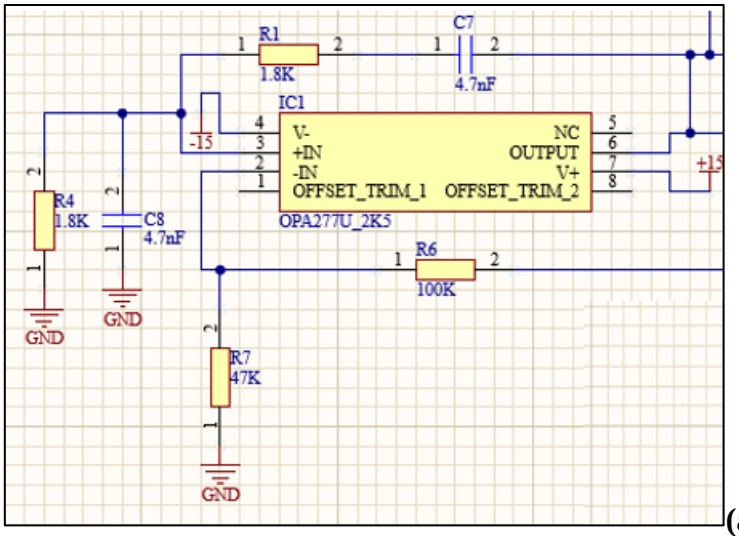

(a)

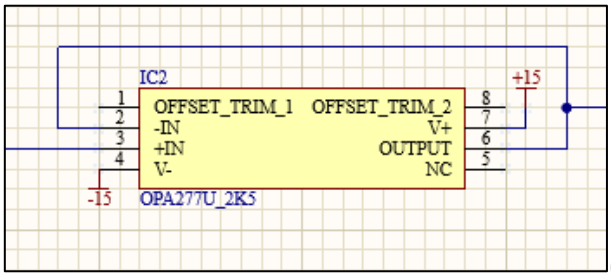

(b)

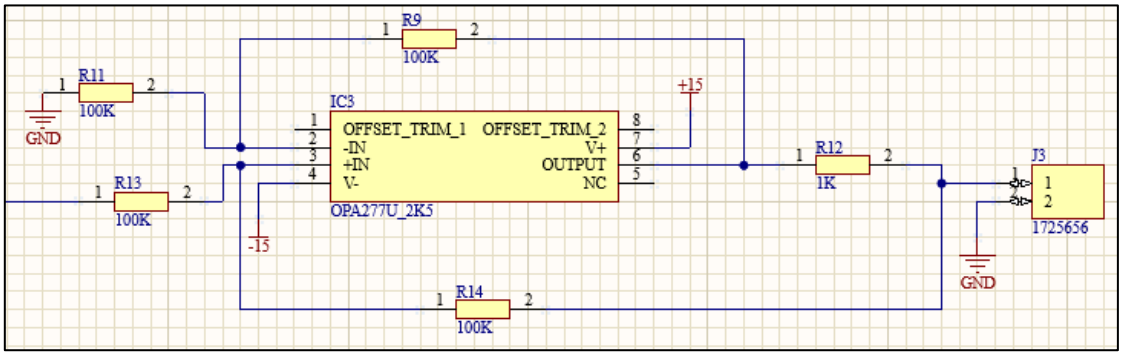

(c)

Figure 3.7 Schematic diagram of injection section of circuit (a) Oscillator Circuit (b) Buffer circuit (c) Voltage to Current converter circuit

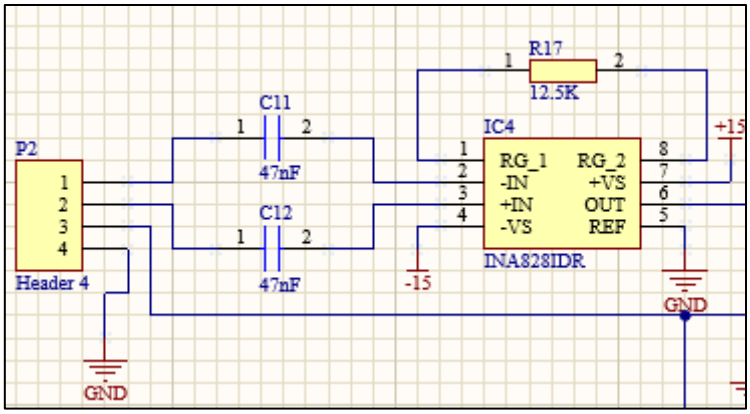

Figure 3.8 Schematic diagram of measurement section of circuit

3.4.2 Develop printed circuit board

Now that the circuit schematic has been developed, one can go ahead and start developing the printed circuit board. In general, the process involves at first, to arrange all the components in a way the components that are connected to each other are close to one another, while saving as much space as possible. Then, one must wire all the components as described in the schematic that was just developed. In Figure 3.9 one can observe the developed printed circuit board's 3D view.

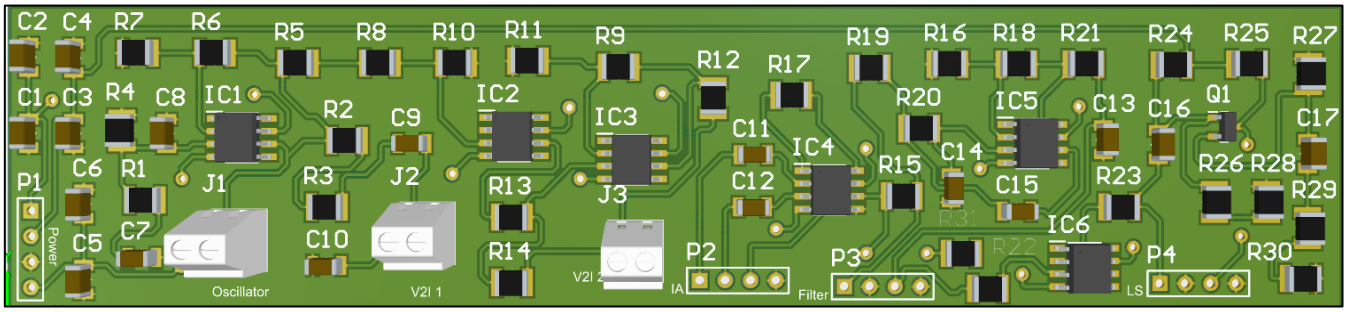

Figure 3.9. 3D view of developed bioimpedance PCB

The developed PCB spans a measurement of 13.4 cm by 3.04 cm. It contains an oscillator, buffer, voltage to current converter and instrumentation amplifier. It also has some filters added but they were not utilized at this stage. Each stage has a connector

represented by the white blocks to test all the different sections and ensure correct functionality.

3.4.3 Test circuit

To assess the design, a test subject will obtain bioimpedance signal from the developed printed circuit board to ensure one can still obtain bioimpedance signal similar in morphology to what was obtained before. This was carried out by connecting the electrodes in the selected Wenner configuration and placed on top of the artery.

In Figure 3.10, the data obtained from the circuit is presented. Signal processing was done in MATLAB to extract the desired bioimpedance signal, as well as a 6 Hz lowpass filter. One can observe the obtained signal from the developed printed circuit board a well as the 1^{st} derivative of the signal. It can be seen that the morphology of the obtained bioimpedance signal is similar to the one obtained previously with the breadboard and with the Biopac machine. Hence, one can go ahead and continue to the next part of the circuit development.

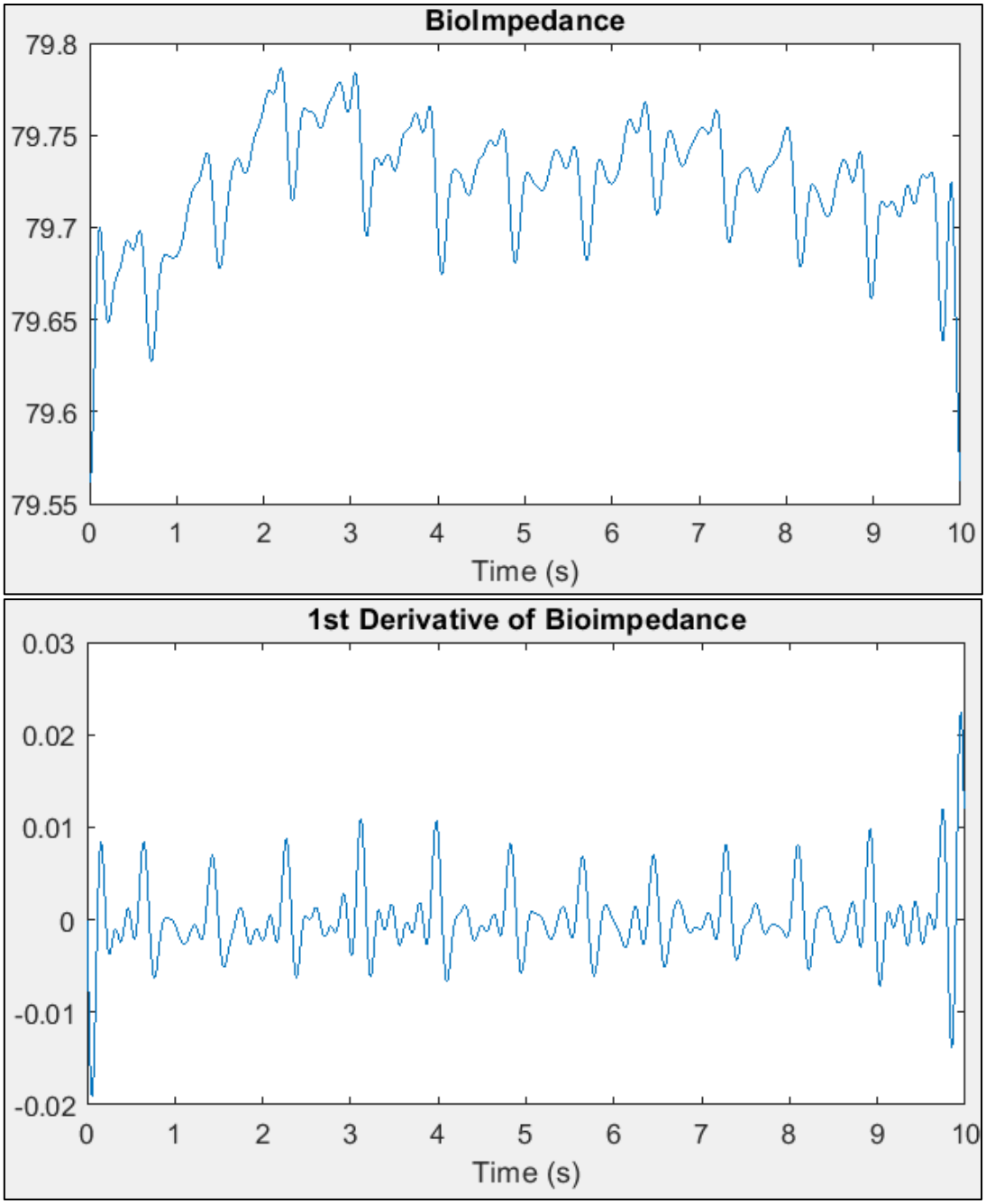

Figure 3.10. Bioimpedance signal from PCB after computer processing, and 1st derivative

4. REDESIGN AND ADDITION OF SIGNAL PROCESSING TO CIRCUIT

4.1 Approach

After the injection section and the measurement section of the bioimpedance printed circuit board have been proven to function correctly and are capable of obtaining bioimpedance signal, one can start making and testing the third section of the bioimpedance circuit. The purpose of adding this section to the circuit is so that one can obtain the signal of interest directly as the output of the circuit rather than having to do signal processing of the signal in a computer. Also, addition of on-board signal processing allows the sampling rate to be decreased significantly from 100 kHz to ~100 Hz, which decreases the amount of data to be captured and increases the capability of the system to acquire data for longer periods of time.

4.2 Literature search on amplitude demodulation

After injecting a current into the tissue, physiological body processes such as the beating of the heart and a person's respiration modulate the amplitude of the generated voltage across the tissue [36]. Because of this, it is necessary to understand thoroughly how amplitude modulation and demodulation works, to be able to implement it in the circuit.

In modulation, there are two types of signals: a carrier signal, and an information signal [37]. A carrier is typically a single frequency signal which serves to, as its name mentions, carry another signal. The information signal will modify some aspect of the carrier signal. For amplitude modulation, the information signal modifies only the amplitude of the carrier signal and keeps its frequency intact. Generally, the amplitude and frequency of the carrier signal are greater than those of the information signal. In Figure

4.1, one can observe the representation of a carrier signal = $\sin(2\pi 25t)$, an information signal = $0.3\cos(2\pi 2t)$, and the resultant amplitude modulated signal:

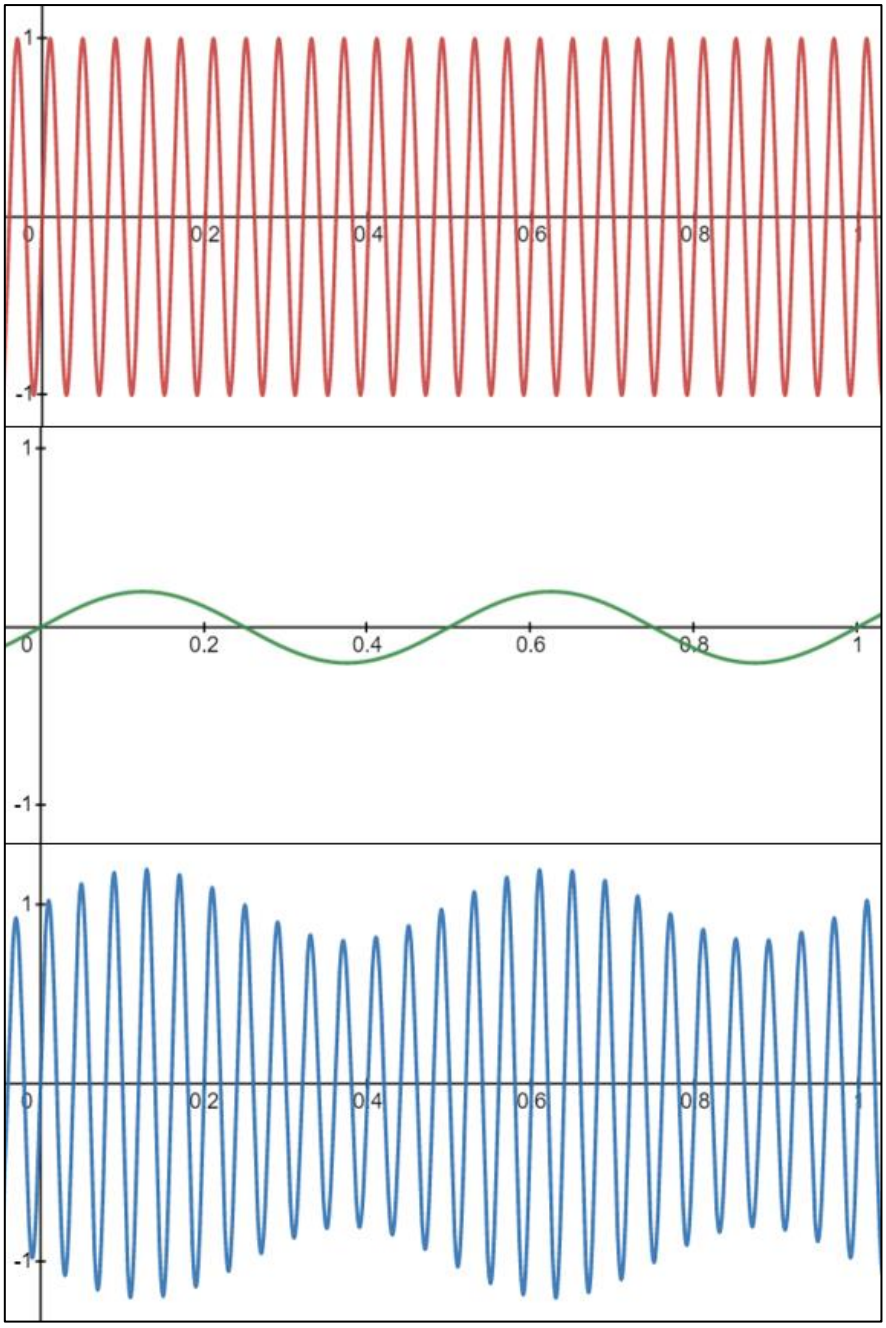

Figure 4.1. Top: Carrier Signal, Middle: Information Signal, Bottom: AM Signal, all in time domain

It can be observed how the amplitude modulated signal still has its original frequency, but its amplitude varies according to the shape of the information signal. Looking at it from a mathematical perspective, one can represent the carrier signal and the information signal as follows:

$$c(t) = a_c \sin(\omega_c t)\,, i(t) = a_i \cos(\omega_i t)$$

Here, $c(t)$ is the carrier signal, a_c is the amplitude of the carrier signal and ω_c is the frequency of the carrier signal. Then, $i(t)$ is the information signal, a_i is the amplitude of the information signal and ω_i is the frequency of the information signal. a_i itself can be represented as ka_c. Then, one can obtain the modulated signal $y(t)$ by multiplying the carrier by $\left[1 + \frac{i(t)}{a_c}\right]$:

$$y(t) = \left[1 + \frac{i(t)}{a_c}\right] c(t) = \left[1 + \frac{a_i \cos(\omega_i t)}{a_c}\right] c(t) = [1 + k\cos(\omega_i t)] c(t)$$

$$y(t) = a_c \sin(\omega_c t) + k\cos(\omega_i t)\, a_c \sin(\omega_c t)$$

Using a trigonometrical product identity, one then obtains:

$$y(t) = a_c \sin(\omega_c t) + 0.5 k a_c \left[\sin\big((\omega_c + \omega_i)t\big) + \sin\big((\omega_c - \omega_i)t\big)\right]$$

It can be observed that the modulated signal, contains three frequency components, its original carrier frequency, one upper sideband from the addition of the carrier and information frequencies and a lower sideband from subtracting the information frequency from the carrier frequency. In Figure 4.2, one can observe the carrier, information, and modulated signals in the frequency domain, using the same example from above.

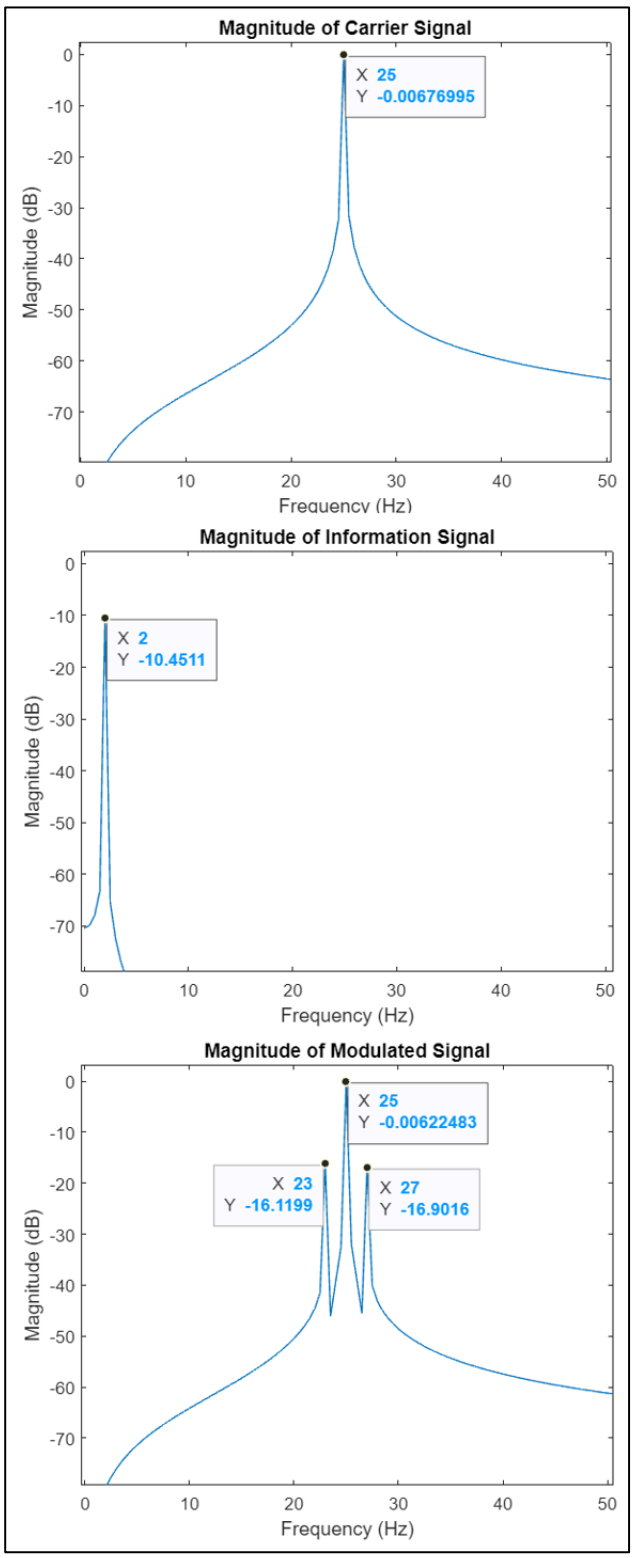

Figure 4.2. Top: Carrier Signal, Middle: Information Signal, Bottom: AM Signal, all in frequency domain

One can observe in the carrier image, how there is a peak at the chosen frequency of 25 Hz, and also in the information image, there is a peak at 2 Hz. Obtaining the magnitude of the frequency response of the modulated signal generates the image in the bottom. One can observe how there are three main peaks present in the frequency spectrum, one at 23 Hz, one at 25 Hz, and one at 27 Hz.

For our case, like mentioned before, the carrier signal is generated by the circuit being developed. The information signal, is artery pulsation information coming from the heart beating and also respiration information from motion. The way it works is that whenever the carrier signal is injected into the body on top of an artery, the artery pulsation will modify the amplitude of the carrier signal, generating the amplitude modulated signal. In the frequency spectrum, like showed in Figure 4.2, before interacting with the body, the carrier signal has one main peak at its frequency, ~19 kHz in our case. After being modulated, it will also contain on each side the frequency components related to the artery and respiratory processes. It is because of this reason, that an amplitude demodulation circuit is required, so that the signal of interest can be extracted from the high frequency carrier signal.

To understand how to demodulate a signal to obtain the low frequency components of interest, one can first look at it from a mathematical point of view. This will be done by taking the previously obtained modulated signal $y(t)$, squaring it, and then simplifying it:

$$y(t) = a_c \sin(\omega_c t) + 0.5ka_c\left[\sin\left((\omega_c + \omega_i)t\right) + \sin\left((\omega_c - \omega_i)t\right)\right]$$

$$y^2(t) = \left\{ a_c \sin(\omega_c t) + 0.5ka_c\left[\sin\left((\omega_c + \omega_i)t\right) + \sin\left((\omega_c - \omega_i)t\right)\right] \right\}^2$$

$$y^2(t) = a_c^2 \sin^2(\omega_c t) + a_c^2 k \sin(\omega_c t)\,[\sin(\omega_c + \omega_i)t + \sin(\omega_c - \omega_i)t]$$
$$+ 0.25k^2 a_c^2 \sin^2(\omega_c + \omega_i)t + 0.5k^2 a_c^2 \sin(\omega_c + \omega_i)t * \sin(\omega_c - \omega_i)t$$
$$+ 0.25k^2 a_c^2 \sin^2(\omega_c - \omega_i)t$$

$$\sin a \sin b = 0.5\cos(a - b) - 0.5\cos(a + b)$$

$$y^2(t) = 0.5a_c^2(1 - \cos 2\omega_c t) + 0.5a_c^2 k(\cos \omega_i t - \cos(2\omega_c t + \omega_i t))$$
$$+ 0.5a_c^2 k(\cos \omega_i t - \cos(2\omega_c t - \omega_i t))$$
$$+ 0.125k^2 a_c^2(1 - \cos(2\omega_c t + 2\omega_i t)) + 0.25k^2 a_c^2(\cos 2\omega_i t - \cos 2\omega_c t)$$
$$+ 0.125k^2 a_c^2(1 - \cos(2\omega_c t - 2\omega_i t))$$

$$y^2(t) = [0.5a_c^2 + 0.25k^2 a_c^2] + [a_c^2 k]\cos \omega_i t + [0.25k^2 a_c^2]\cos 2\omega_i t$$
$$- [0.125k^2 a_c^2]\cos(2\omega_c t - 2\omega_i t) - [0.5a_c^2 k]\cos(2\omega_c t - \omega_i t)$$
$$- [0.5a_c^2 + 0.25k^2 a_c^2]\cos 2\omega_c t - [0.5a_c^2 k]\cos(2\omega_c t + \omega_i t)$$
$$- [0.125k^2 a_c^2]\cos(2\omega_c t + 2\omega_i t)$$

The modulated signal itself only has three frequency components: ω_c, $\omega_c + \omega_i$, and $\omega_c - \omega_i$. The reason the signal is squared is so that one can obtain the frequency component of interest by itself. As observed, after squaring the modulated signal, one obtains eight frequency components, but most importantly, one obtains $[a_c^2 k]\cos \omega_i t$ which is the frequency of the original information signal. Hence, one can say that to demodulate the modulated signal, one can just square the modulated signal. In Figure 4.3, one can observe the magnitude frequency spectrum of the squared signal for the example from Figure 4.2.

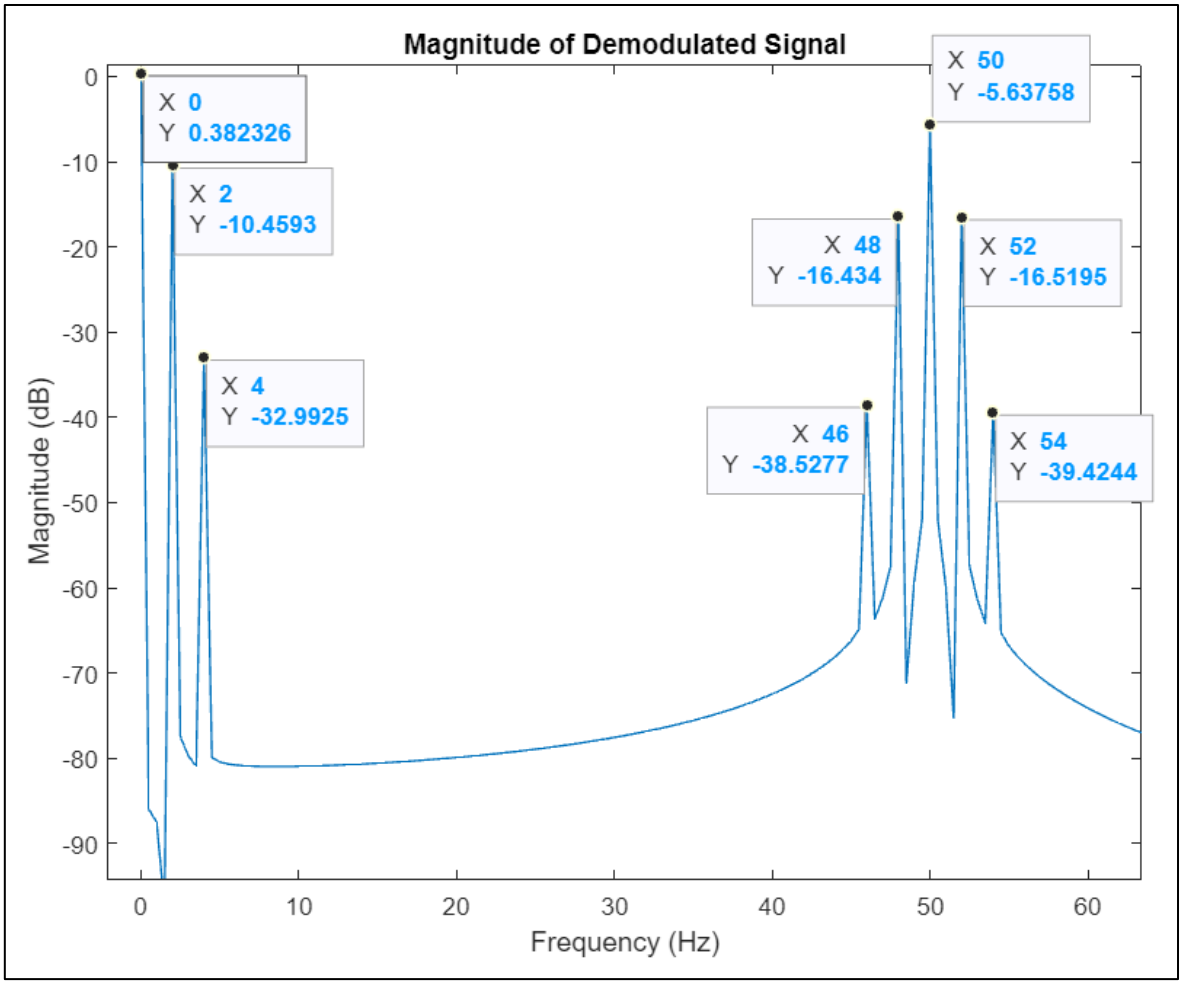

Figure 4.3. Magnitude frequency spectrum of demodulated signal

One can observe how there are eight peaks at different frequencies, just as what was obtained previously for $y^2(t)$. However, more importantly, we are able to obtain the original frequency signal, which for this case was 2 Hz. Hence, a circuit component is needed that is capable of multiplying the input signal and generating as output the demodulated signal. Additionally, one will require the addition of an analog lowpass filter to eliminate the additional higher frequencies generated during the demodulation of the signal. This will allow us to obtain as output from the circuit the information signal, along with some additional DC component.

4.3 Component selection and test circuit

4.3.1 Amplitude demodulation

For this section, one must use a demodulation circuit component which fits our application. That means, finding a demodulation chip which is capable of running in the kilohertz frequency range. For this, there are not many options available since most demodulation chips are made for the telecommunications industry which utilizes the GHz frequency band. In fact, there is only one such commercially feasible chip that can perform amplitude demodulation while still being appropriate for our application, which is the AD630. This is a high precision chip which is capable of demodulating a signal while still working efficiently in the kHz range of frequencies.

4.3.2 Analog filters

A high pass filter at 0.1 Hz will be used to eliminate unwanted low frequency signals coming from the output of the instrumentation amplifier. Additionally, a low pass filter at 10 Hz will be used to eliminate unwanted high frequencies such as high frequency residuals from the multiplying circuit within the demodulator. The circuit will then be tested to ensure that bioimpedance signal can be obtained without having to perform amplitude demodulation in the computer and while sampling at a low frequency such as 250 Hz or lower. If this is successful, one can go ahead and start developing the printed circuit board.

4.3.3 Test circuit

In Figure 4.4 one can observe the signal obtained after testing the addition of the AD630 demodulator and the mentioned filters. There was an additional lowpass filter to process the signal in MATLAB at 3.5 Hz. It can be seen that the signal has the same

morphology as what is expected for bioimpedance, hence, one can go ahead and build the printed circuit board with the newly added components.

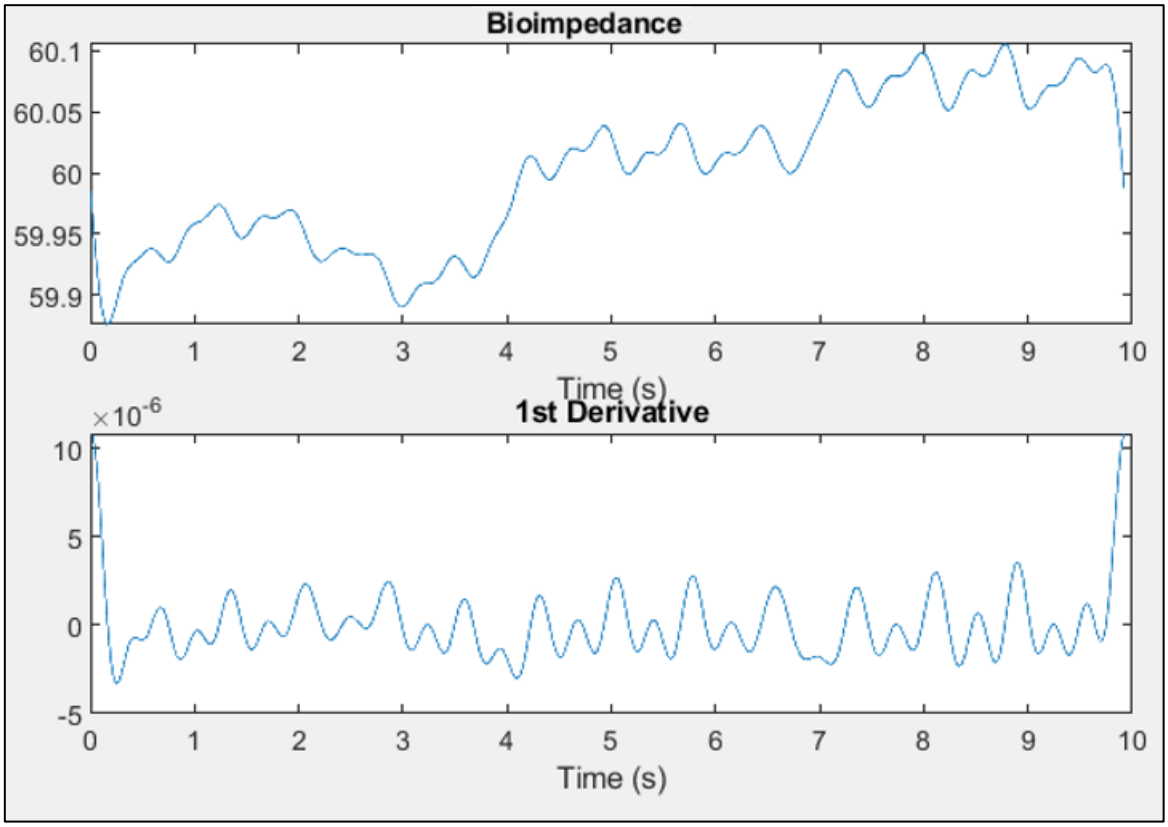

Figure 4.4. Bioimpedance signal obtained with modified breadboard circuit

4.4 Develop schematic, printed circuit board and test circuit

4.4.1 Develop schematic

After it is determined that the previous circuit, now with the addition of the signal processing and demodulation components, is working as expected, the new printed circuit board will be developed. For this, the added filters, as well as the demodulation chip, will be added to the previous Altium schematic. The OPA277 amplifier was replaced by the OPA4191 since it is smaller in size and it has four operational amplifiers in one. Additionally, the INA828 was replaced by the AD8222 instrumentational amplifier since

its size is smaller. One can observe Tables 4.1 and 4.2 that the electrical characteristics of the new components are similar to the previously selected components [38, 39].

Table 4.1: Electrical characteristics for OPA4191

Parameter	**Typical Value**	**Unit**
Input Voltage Noise Density	12	nV/√Hz
Common Mode Rejection	60	dB
Open loop gain	50	dB

Table 4.2: Electrical characteristics for AD8222

Parameter	**Typical Value (for G = 10)**	**Unit**
Input Voltage Noise Density	16	nV/√Hz
Common Mode Rejection	90	dB

The new schematic file will then be made by adding the new components and connecting them to the rest of the circuit components. In Figure 4.5, one can observe the developed schematic with the new components.

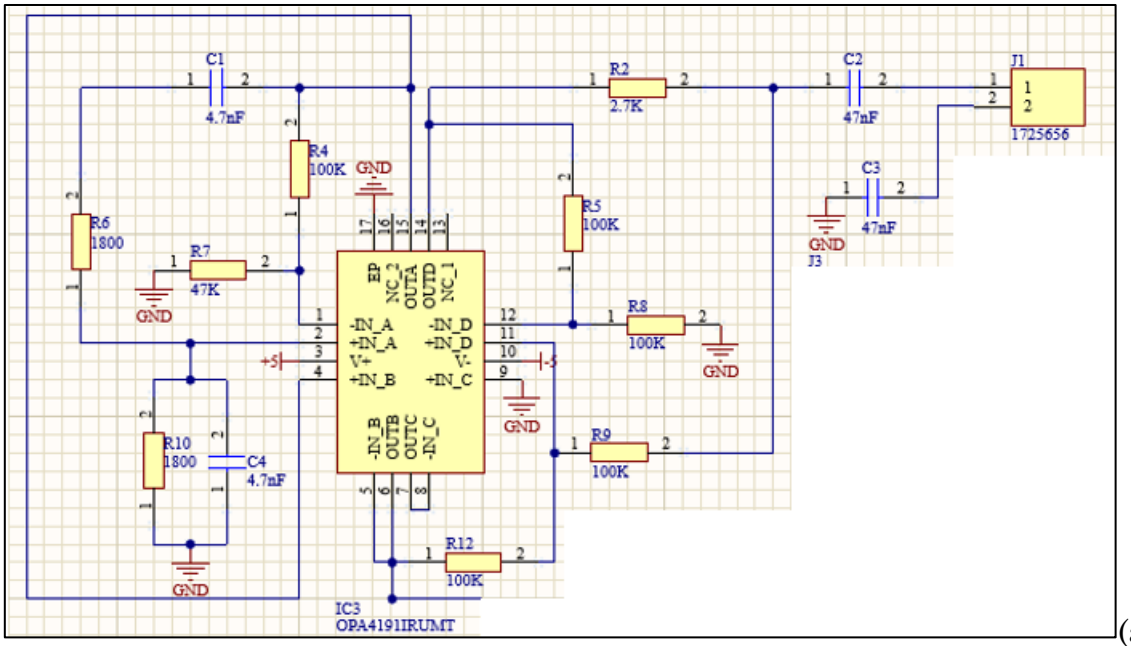
C1
4.7nF
R2
2.7K
C2
47nF
J1
1725656
R4
100K
GND
C3
47nF
R5
100K
R6
1800
R7
47K
R8
100K
R9
100K
R10
1800
C4
4.7nF
R12
100K
IC3
OPA4191IRUMT
(a)

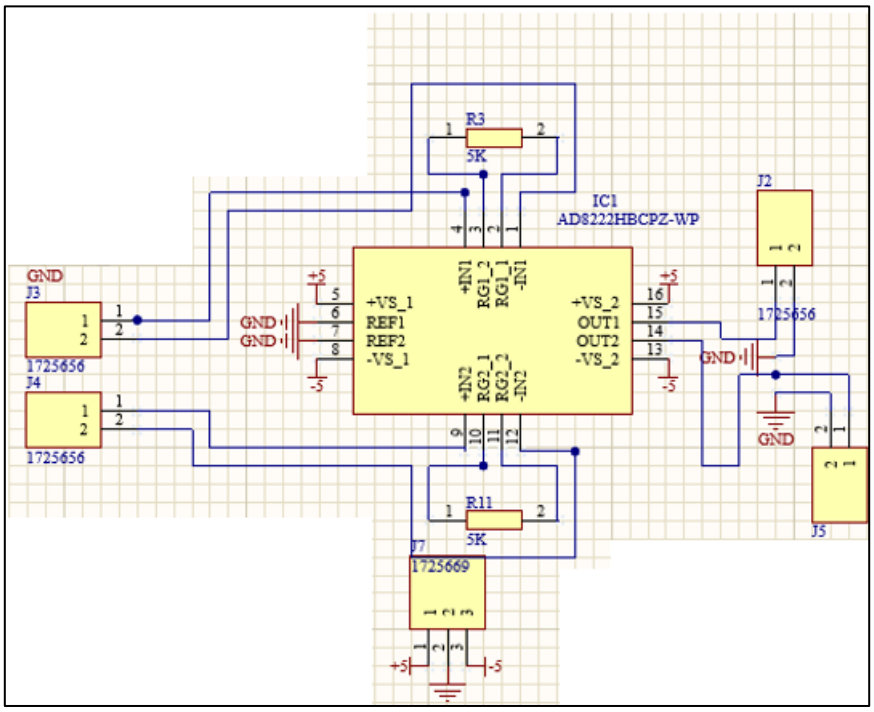
R3
5K
IC1
AD8222HBCPZ-WP
J2
1725656
J3
1725656
J4
1725656
R11
5K
J7
1725669
J5
(b)

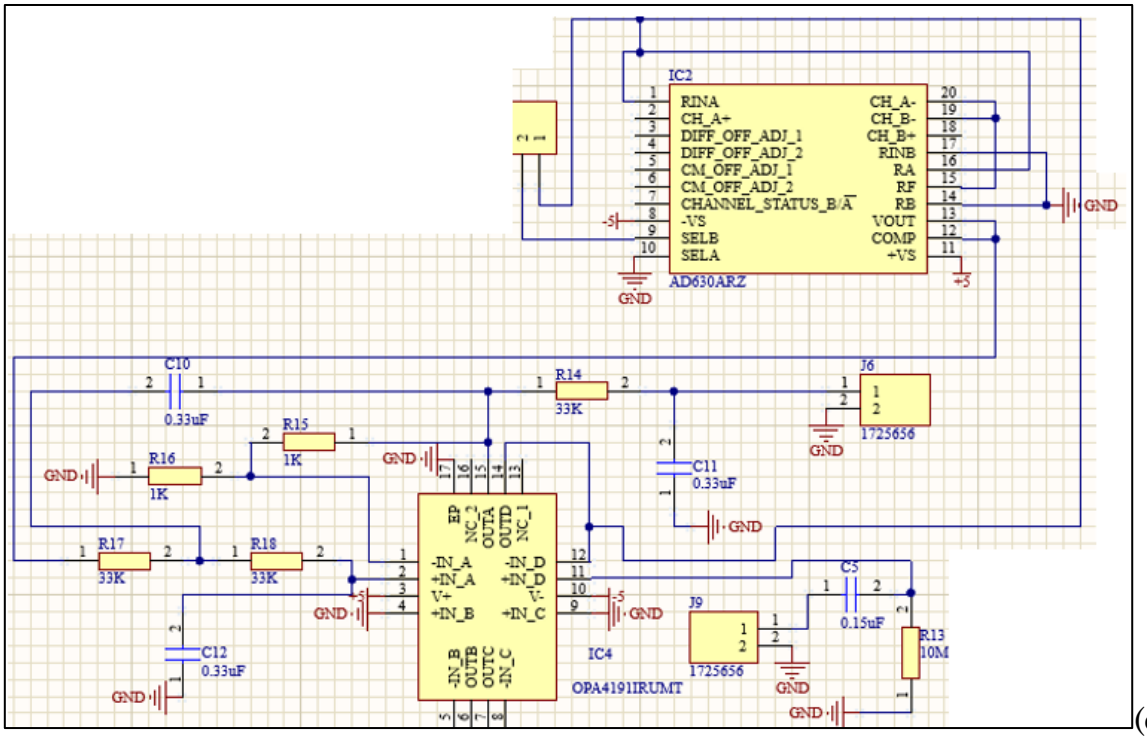

(c)

Figure 4.5 Schematic diagram of circuit with processing components added: (a) Oscillator, Buffer, and Voltage to Current converter circuit (b) measurement circuit (c) Demodulator and analog filters

4.4.2 Develop printed circuit board

Now that the circuit schematic has been developed, one can go ahead and start developing the printed circuit board. Again, all the components are arranged in a functional way, while still saving space. Then, all the components are wired as described in the schematic that was just developed. In Figure 4.6, one can observe the 3D view of the printed circuit board developed.

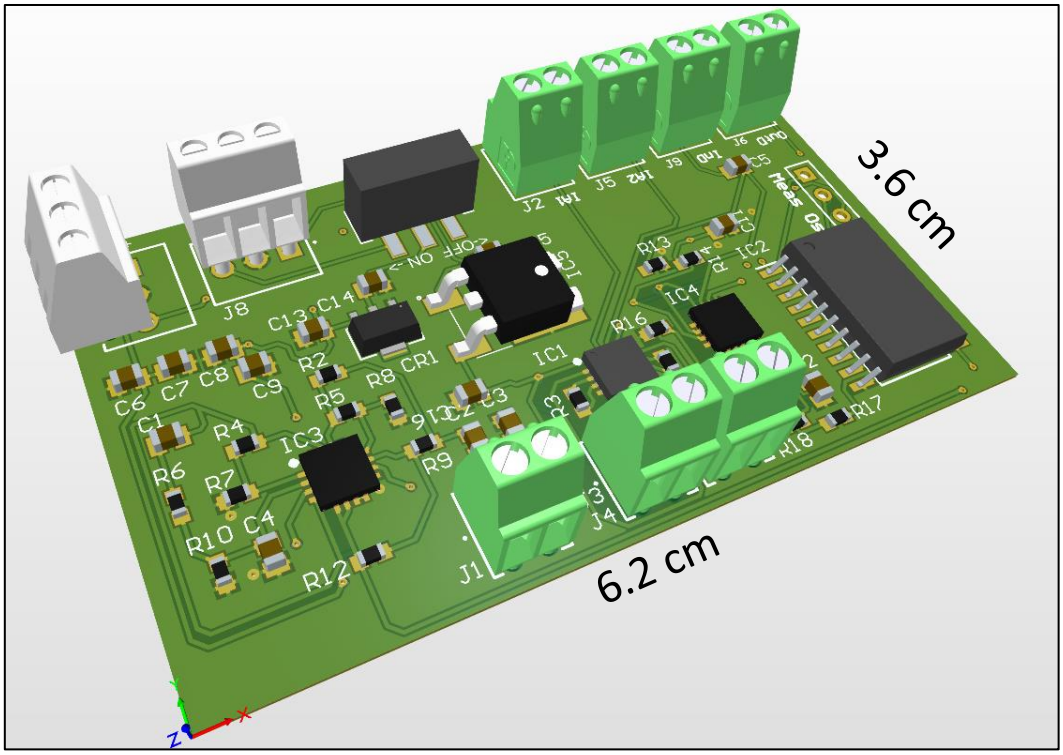

Figure 4.6. 3D view of final developed bioimpedance PCB

The developed PCB spans a measurement of 6.2 cm by 3.6 cm. It contains an injection section, a measurement section, and a signal processing section. The system needs $\pm 5V$ to power the circuit. To run the system using 9V batteries, power regulator components were added to step the voltage down appropriately. Additionally, a mechanical switch was added to turn the circuit on and off as needed. The white connectors are used for powering the circuit and the green connectors are for input and output connectivity. The circuit was then printed and the components were soldered for testing the system.

4.4.3 Test circuit

Once the new PCB arrived, it was tested to obtain bioimpedance signal and ensure that the morphology is similar to what has been obtained before. In Figure 4.7, a flow chart of the full system can be observed to better visualize how the data collection process will

work for the full system and in Figure 4.8, the data collected from the final PCB can be observed.

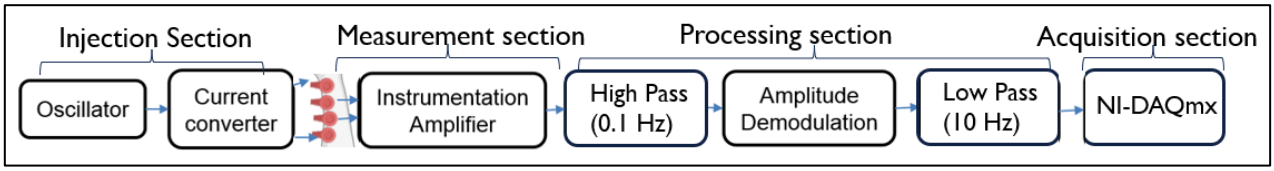

Figure 4.7. Flow chart for bioimpedance circuit data acquisition

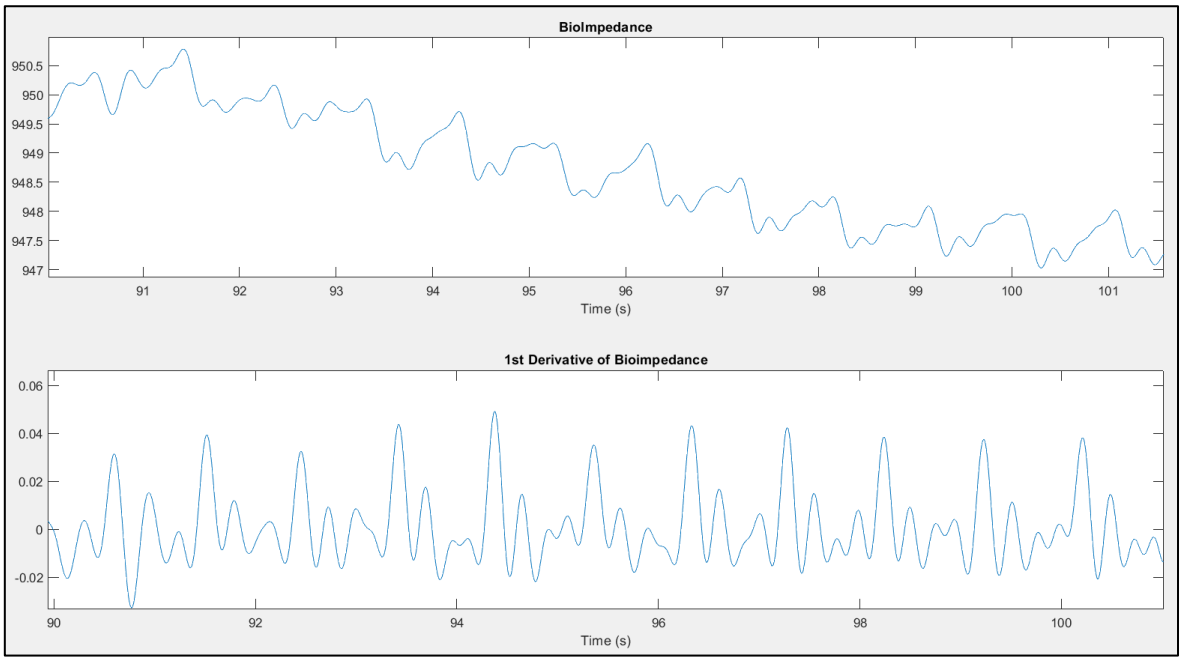

Figure 4.8. Bioimpedance signal collected from final PCB

Now that bioimpedance signal can be collected with the final PCB, one needs to calibrate the measurements so we can see real impedance values. The scale in Figure 4.8 is modified because of all the digital and analog gains and filtering. To calibrate the system, measurements were taken with the PCB for different resistor values as observed in Figure 4.9.

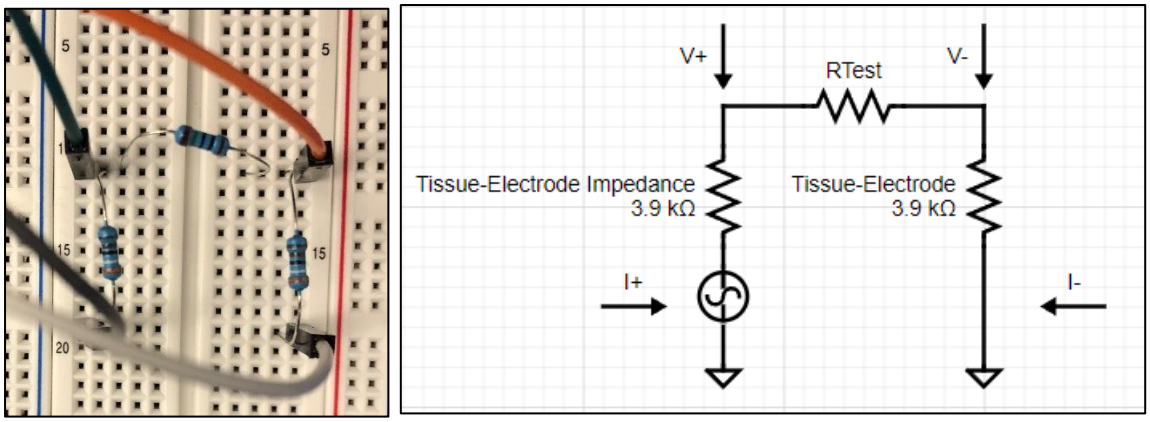

Figure 4.9. System Callibration Setup

As observed in Figure 4.9, to calibrate the system, three resistors were needed, two resistors that simulate the tissue electrode impedance and one resistor whose value will change. Typical tissue-electrode impedance values for wet electrodes are around the low kΩ range, so 3.9 $k\Omega$ resistors were chosen [40]. The current generated by the circuit is injected at the bottom into each resistor. Then, the voltage measurement component of the circuit will measure the voltage differential generated across RTest. For each value of RTest, data was collected for a minute and the voltage value obtained was averaged over that minute. This was done for four resistance values: $15\ \Omega, 68\ \Omega, 100\ \Omega,$ and $150\ \Omega$. In Figure 4.10, one can observe the plot generated of the voltage obtained by the circuit as a function of the input resistance.

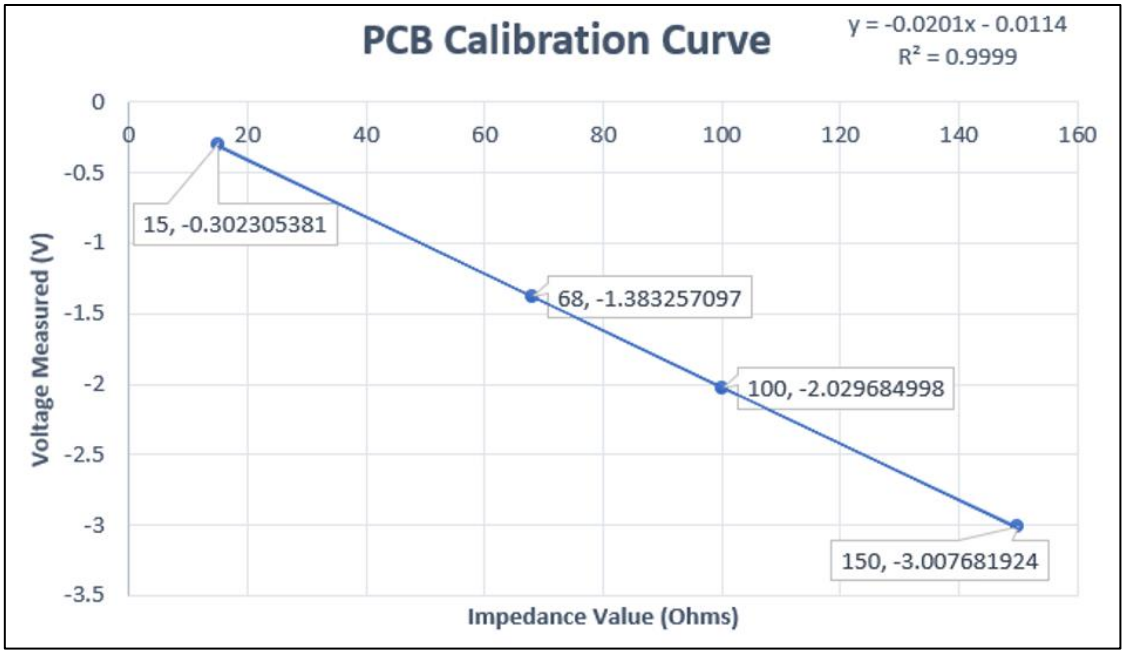

Figure 4.10. PCB Calibration Curve

The relationship obtained between the input resistance value and the output measured voltage is linear and highly correlated. The functional relation is obtained as $y = -0.0201x - 0.0114$ where x is the resistance value and y is the measured voltage. For our purposes, the conversion desired is from measured voltage to resistance value, so the inverse function is required, that is: $x = \frac{y+0.0114}{-0.0201}$. Now that the system works properly and the system is calibrated to obtain resistance values, one can go ahead and compare the finished system to a gold standard.

5. COMPARISON OF DEVELOPED CIRCUIT VERSUS GOLD STANDARD

5.1 Approach

Once that the PCB with all three circuit sections is working properly and that the system has been calibrated, the next step is to compare the developed circuit to a commercial device. The test will consist of a person wearing three devices simultaneously to obtain physiological signals from all devices. Then, after signals are obtained from the three devices, heart rate and respiration rate will be calculated for each of them. Finally, one will conclude whether the obtained values from the developed PCB are close to the ones obtained from the other two devices. The full process for data collection and processing is graphically explained in Figure 5.1. The bandpass filter is 0.5 – 6.5 Hz.

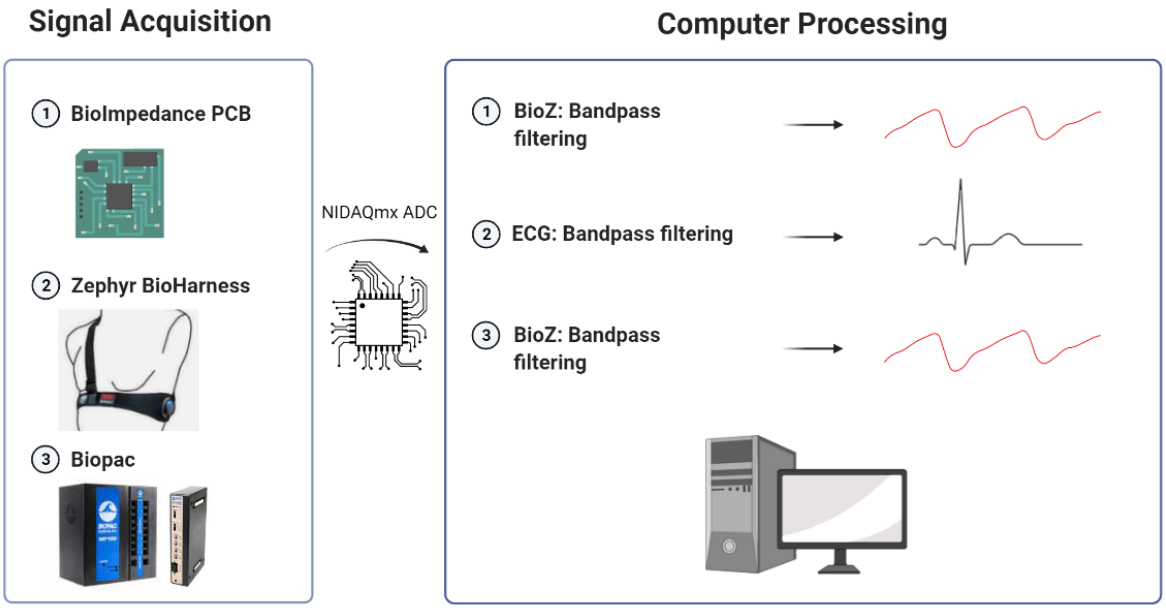

Figure 5.1. Data collection and processing process

5.2 Data collection with developed PCB and commercial device simultaneously

Before starting to collect data, one needs to determine the best location to place the electrodes. This is done by utilizing electrode gel and a handheld ultrasound monitor

(Sonotrax Vascular Doppler) and placing it on different places around the inner side of the upper arm. The brachial artery is located in between the biceps brachii and the triceps brachii so that is a good place to start looking. Once the locations are found, they will be marked using surgical-grade skin-safe markers from Viscot (™) and then the electrodes can be placed on the subject's skin. The developed bioimpedance circuit collected data from the left arm as observed in Figure 5.2. The research grade bioimpedance machine collected data from the right arm as observed in Figure 5.3.

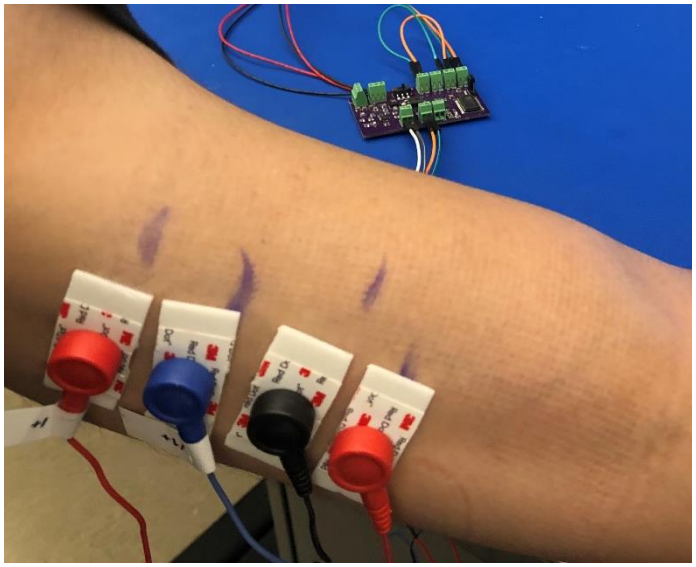

Figure 5.2. Electrode location in right upper arm

Figure 5.3. Electrode location in left upper arm

At the same time, under the shirt, the subject is wearing a Zephyr BioHarness device which can capture ECG, heart rate and respiration rate. For data collection, the person will be sitting, and an armband will be placed around the upper arm as observed in Figure 5.4 so the electrodes can be as close as possible to the brachial artery. In Figure 5.5, one can observe the printed circuit board being powered with 9V batteries for data collection.

Figure 5.4. Example of subject setup for data collection

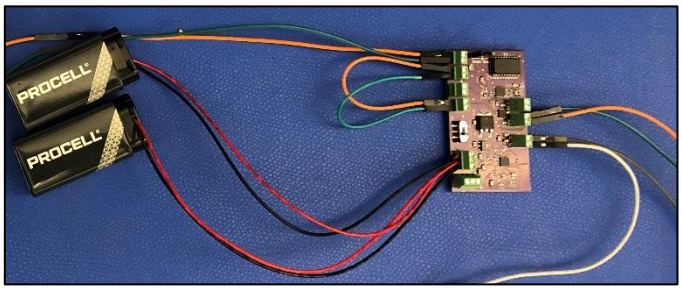

Figure 5.5. Printed circuit board setup for data collection

Data was collected from all three sensors simultaneously in five situations: sedentary, sedentary with paced respiration, typing, typing with paced respiration, and sedentary, one minute each. Of the described process, two trials were collected for each subject, having three subjects in total. For the paced breathing situations, a phone app was used so the subject would follow and maintain 10 respirations per minute. Once data was collected from the devices, data processing and analysis of it was performed.

5.3 Perform signal processing and compare systems

After signal was collected from all sensors in the mentioned manner, they were further processed in the computer with a 0.5 – 6.5 bandpass filter to remove any residual high and/or low frequency noise. Data collected from one trial is shown in Figure 5.6 to show an example of how it looks like. Also, a closeup after removing the baseline is shown in Figure 5.7 to appreciate the bioimpedance signal itself:

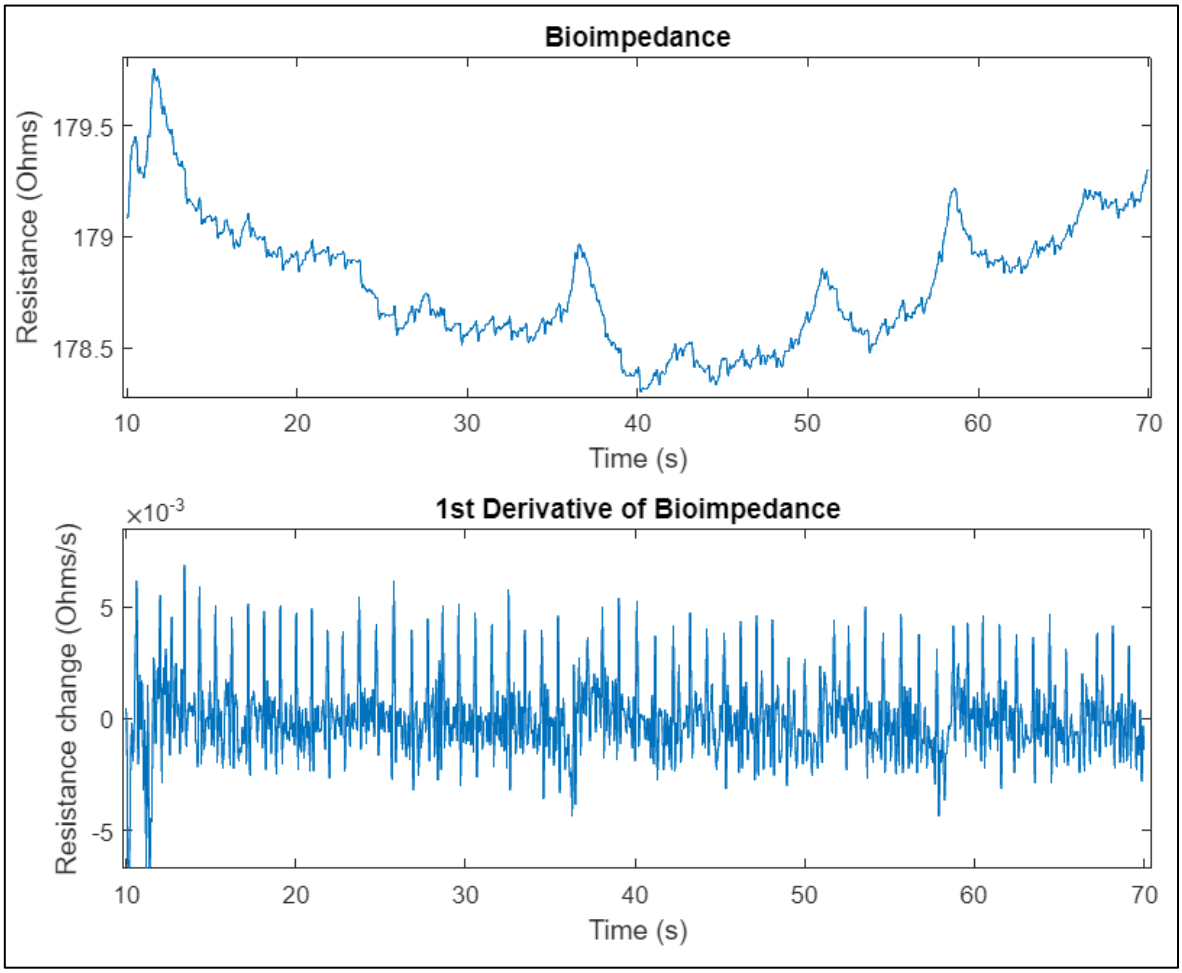

Figure 5.6. Data collection from developed bioimpedance system for one trial

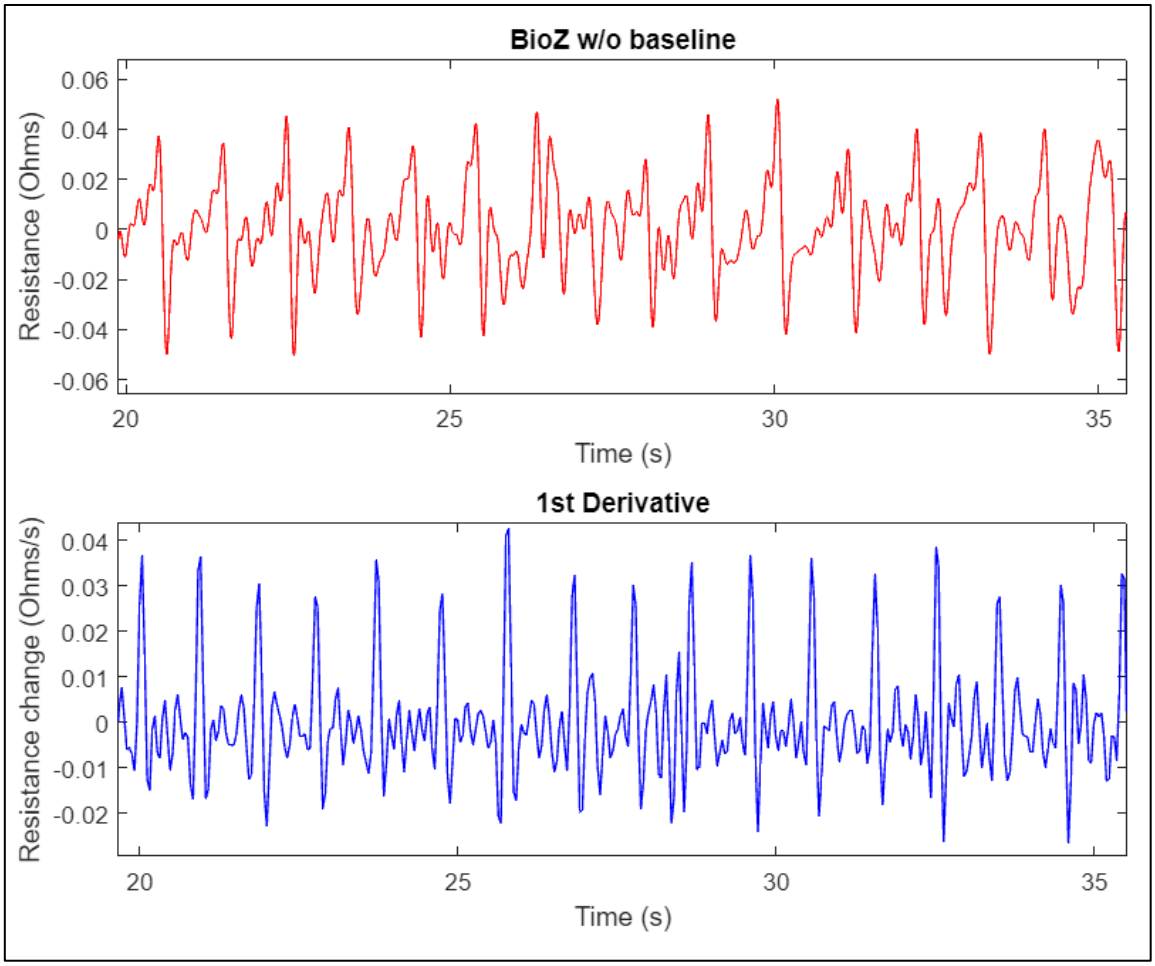

Figure 5.7. Closeup of collected bioimpedance signal after removing baseline

On Figure 5.8, one can observe the electrocardiography data obtained from the Zephyr device and in Figure 5.9 a closeup of the obtained data. Heart rate was calculated in the same way for both systems so that they can be compared in a fair manner. Additionally, in Figure 5.10 one can observe bioimpedance signal from the Biopac device as well as a closeup of the signal in Figure 5.11. Finally, depending on the results obtained, one will determine the feasibility of the developed bioimpedance sensing circuit for obtaining vital signs.

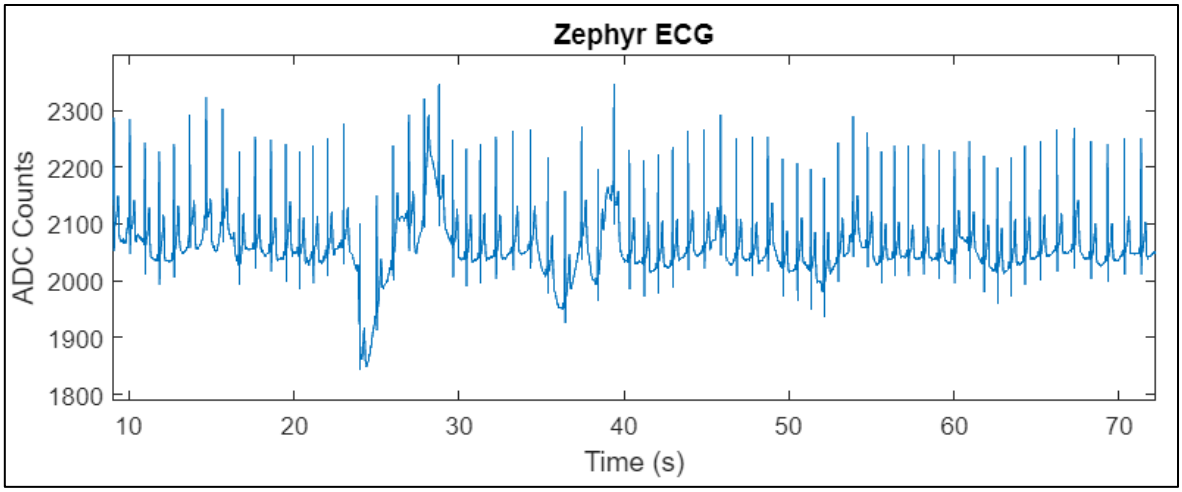

Figure 5.8. Electrocardiography signal obtained from Zephyr device

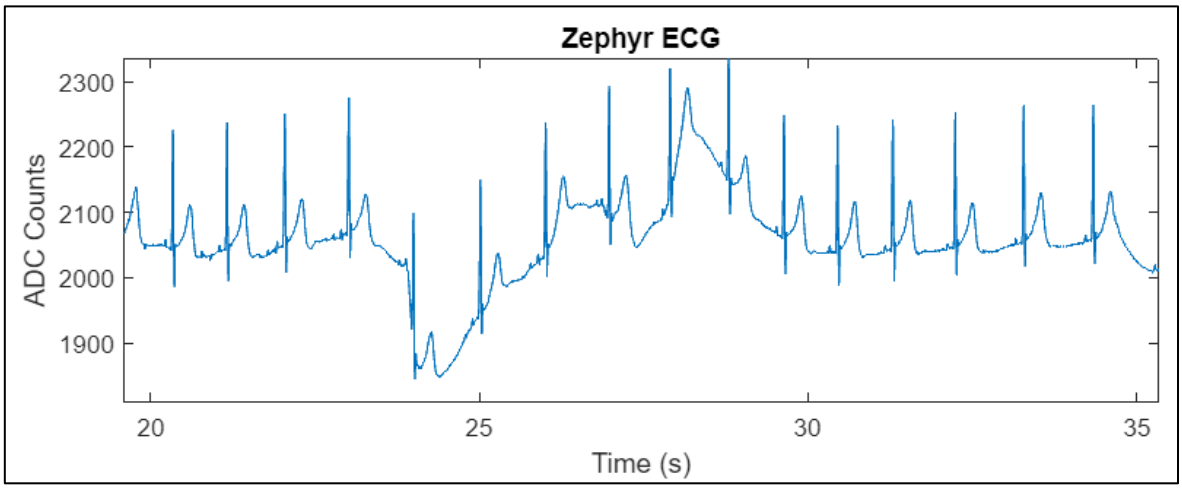

Figure 5.9. Closeup of collected electrocardiography signal from Zephyr device

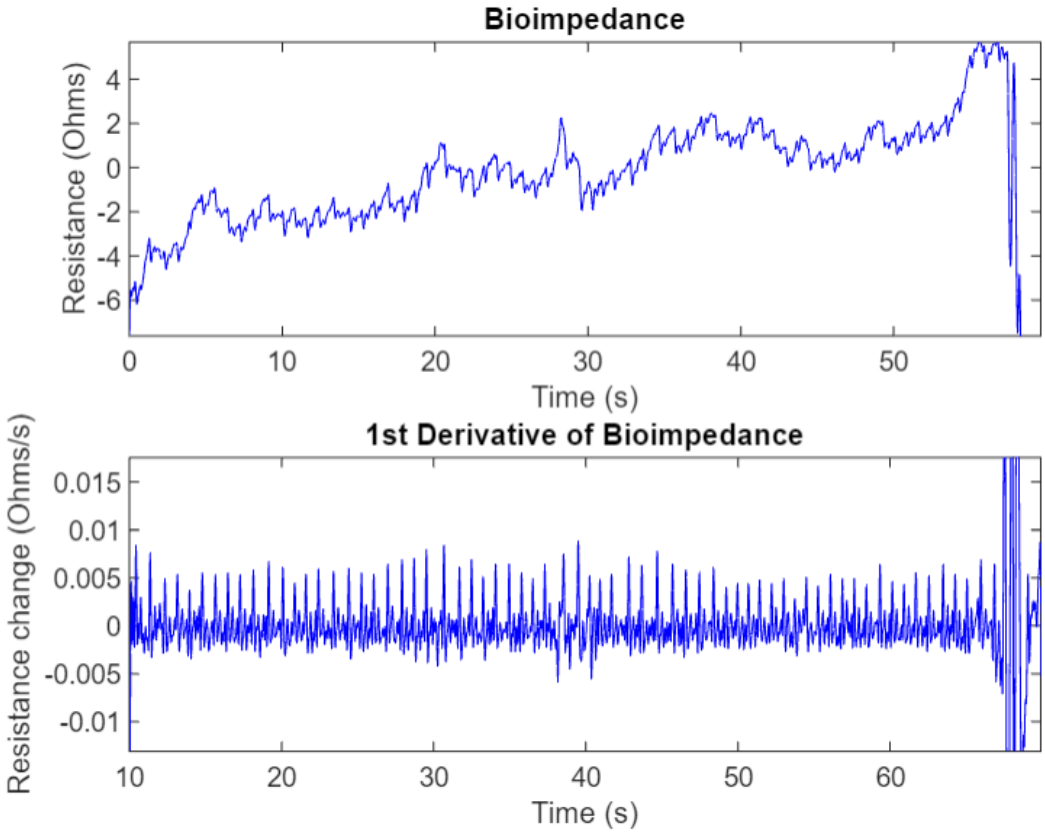

Figure 5.10. Data collection from Biopac system for one trial

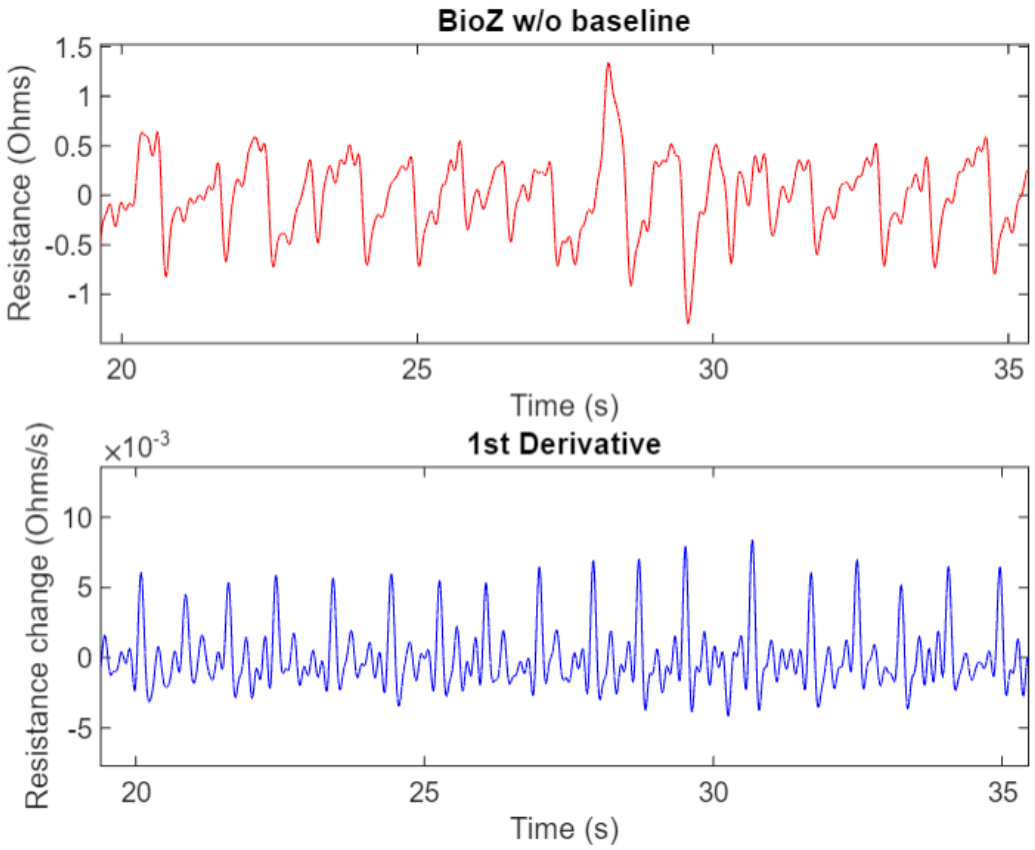

Figure 5.11. Closeup of collected Biopac bioimpedance signal after removing baseline

In Tables 5.1 – 5.6, one can observe the comparison of the heart rate and respiration rate values obtained for each test subject for the different conditions tested. The heart rate and respiration rate values were obtained using functions from a Python library called NeuroKit2 which is specialized for physiological signal processing [41].

Table 5.1: Heart Rate Results for Subject 1

Subject 1	**PCB Heart Rate (bpm)**	**Zephyr Heart Rate (bpm)**	**Biopac Heart Rate (bpm)**
Sedentary T1	78.6 ± 1.2	76.5 ± 3.6	76.5 ± 5.2
Sedentary Respiration T1	72.8 ± 2.1	73.4 ± 4.5	72.7 ± 8.4
Typing T1	101.3 ± 32.1	79.3 ± 6.1	76.2 ± 24.8
Typing Respiration T1	93.8 ± 30.4	83.0 ± 4.7	81.1 ± 21.0
Sedentary T1	78.4 ± 2.7	77.3 ± 5.1	78.0 ± 11.2
Sedentary T2	71.8 ± 0.5	69.5 ± 3.4	69.6 ± 4.6
Sedentary Respiration T2	72.8 ± 6.1	73.3 ± 4.1	74.0 ± 7.4
Typing T2	94.7 ± 29.5	77.9 ± 5.6	76.8 ± 23.4
Typing Respiration T2	90.4 ± 22.1	84.7 ± 3.7	78.9 ± 24.5
Sedentary T2	74.2 ± 6.6	76.0 ± 8.6	74.1 ± 7.4

Table 5.2: Respiration Rate Results for Subject 1

Subject 1	**PCB Respiration Rate (bpm)**	**Zephyr Respiration Rate (bpm)**	**Biopac Respiration Rate (bpm)**
Sedentary T1	NA	16.6 ± 0.5	13.9 ± 6.7
Sedentary Respiration T1	11.7 ± 0.3	14.9 ± 2.3	10.3 ± 2.3
Typing T1	6.5 ± 3.7	9.7 ± 0.8	18.8 ± 6.6
Typing Respiration T1	10.8 ± 2.8	10.9 ± 0.8	17.1 ± 7.9
Sedentary T1	NA	9.4 ± 0.8	4.5 ± 0.9
Sedentary T2	10.4 ± 3.8	15.0 ± 0.9	11.7 ± 3.2
Sedentary Respiration T2	10.4 ± 3.2	14.4 ± 2.3	9.5 ± 0.9
Typing T2	14.0 ± 4.2	10.1 ± 0.9	19.9 ± 11.7
Typing Respiration T2	10.4 ± 3.9	8.3 ± 0.6	23.7 ± 9.3
Sedentary T2	8.9 ± 4.6	9.3 ± 0.7	8.2 ± 1.7

Table 5.3: Heart Rate Results for Subject 2

Subject 2	**PCB Heart Rate (bpm)**	**Zephyr Heart Rate (bpm)**	**Biopac Heart Rate (bpm)**
Sedentary T1	71.5 ± 3.8	71.2 ± 4.1	70.1 ± 1.7
Sedentary Respiration T1	67.8 ± 1.6	67.7 ± 3.8	70.1 ± 1.4
Typing T1	*NA*	69.3 ± 2.6	19.0 ± 19.5
Typing Respiration T1	80.0 ± 31.7	70.3 ± 3.7	34.4 ± 25.7
Sedentary T1	66.2 ± 2.8	68.3 ± 4.7	64.5 ± 1.5
Sedentary T2	67.5 ± 8.4	67.6 ± 3.8	68.2 ± 1.4
Sedentary Respiration T2	67.5 ± 4.0	66.5 ± 3.3	69.3 ± 4.7
Typing T2	92.1 ± 32.5	70.3 ± 2.6	19.0 ± 8.7
Typing Respiration T2	104.5 ± 33.9	72.3 ± 3.5	28.0 ± 21.0
Sedentary T2	72.6 ± 2.7	66.7 ± 4.0	59.4 ± 0.8

Table 5.4: Respiration Rate Results for Subject 2

Subject 2	**PCB Respiration Rate (bpm)**	**Zephyr Respiration Rate (bpm)**	**Biopac Respiration Rate (bpm)**
Sedentary T1	8.1 ± 0.2	10.5 ± 0.5	9.0 ± 1.5
Sedentary Respiration T1	10.1 ± 0.3	9.2 ± 0.4	10.0 ± 0.4
Typing T1	NA	13.9 ± 2.9	16.5 ± 6.9
Typing Respiration T1	9.3 ± 1.6	13.8 ± 1.9	9.8 ± 0.8
Sedentary T1	6.6 ± 0.1	10.1 ± 0.7	7.2 ± 0.9
Sedentary T2	8.2 ± 0.9	9.9 ± 1.0	8.3 ± 1.2
Sedentary Respiration T2	7.3 ± 0.8	9.1 ± 0.6	10.0 ± 0.2
Typing T2	NA	11.5 ± 1.3	14.3 ± 1.6
Typing Respiration T2	8.8 ± 4.6	13.2 ± 0.8	11.0 ± 2.1
Sedentary T2	NA	8.3 ± 0.5	9.6 ± 1.5

Table 5.5: Heart Rate Results for Subject 3

Subject 3	**PCB Heart Rate (bpm)**	**Zephyr Heart Rate (bpm)**	**Biopac Heart Rate (bpm)**
Sedentary T1	68.5 ± 4.8	71.4 ± 3.1	73.2 ± 14.7
Sedentary Respiration T1	68.9 ± 3.2	79.0 ± 5.2	72.4 ± 20.3
Typing T1	81.7 ± 20.4	75.4 ± 3.9	98.1 ± 35.1
Typing Respiration T1	84.9 ± 21.6	77.9 ± 3.0	98.3 ± 29.1
Sedentary T1	74.3 ± 4.7	80.2 ± 4.4	74.8 ± 10.4
Sedentary T2	71.8 ± 3.2	69.7 ± 2.8	70.7 ± 10.8
Sedentary Respiration T2	72.2 ± 2.8	78.7 ± 4.8	76.8 ± 12.8
Typing T2	76.4 ± 22.8	74.8 ± 4.2	105.2 ± 32.9
Typing Respiration T2	91.0 ± 31.9	78.6 ± 3.4	94.4 ± 32.5
Sedentary T2	74.3 ± 3.1	73.9 ± 4.1	72.3 ± 5.7

Table 5.6: Respiration Rate Results for Subject 3

Subject 3	PCB Respiration Rate (bpm)	Zephyr Respiration Rate (bpm)	Biopac Respiration Rate (bpm)
Sedentary T1	16.6 ± 1.3	16.3 ± 0.5	14.5 ± 4.8
Sedentary Respiration T1	10.0 ± 0.3	12.5 ± 2.7	11.0 ± 6.7
Typing T1	14.3 ± 5.6	11.8 ± 1.4	9.7 ± 4.6
Typing Respiration T1	10.1 ± 0.3	8.3 ± 1.3	10.7 ± 3.3
Sedentary T1	13.2 ± 7.2	8.5 ± 1.0	12.1 ± 7.0
Sedentary T2	14.1 ± 6.6	18.3 ± 1.3	15.9 ± 4.3
Sedentary Respiration T2	8.8 ± 1.8	15.4 ± 3.1	8.8 ± 2.0
Typing T2	6.2 ± 2.4	9.8 ± 0.9	11.6 ± 6.9
Typing Respiration T2	9.7 ± 1.0	11.8 ± 1.9	13.6 ± 4.5
Sedentary T2	8.4 ± 5.4	9.4 ± 1.2	6.4 ± 2.3

Looking at the sedentary position and comparing between devices and subjects, one can obtain heart rate values where the means generally fall within one standard deviation of each other. The respiration rate is also similar between systems but less consistent since sometimes you do not obtain a respiration signal from the subject.

For the sedentary position with paced respiration, the heart rate values are also comparable between the three systems. However, now for the respiration rate, one can observe that it is more consistent between systems, and at least for the developed PCB, 10 ± 1 bpm always falls in the value obtained from the NeuroKit2 algorithm.

For the typing situation, one cannot obtain heart rate with the developed PCB or with the Biopac bioimpedance machine. The only one that can obtain heart rate is the Zephyr, since it is ECG based, and it is less sensitive to micromotions such as typing. For the respiration rate again, the only consistent device is the Zephyr. The values obtained for the PCB and Biopac have either large standard deviations or sometimes missing values.

For typing with paced breathing, similar to the previous situation, one cannot obtain heart rate with either device except for the Zephyr. However, now one can actually obtain respiration rates close to 10 bpm for both the developed PCB and the Biopac, besides the Zephyr.

Finally, for the fifth situation which was sedentary again. This was mostly done just to observe how the system will go back to measuring heart rate and respiration rate after experiencing motion from typing. As observed in the values obtained, the results seem to follow that of the first sedentary position.

In Table 5.2, it can be observed that the respiration rate could not be obtained from the PCB for one trial. This greatly depends on the subject and the measurement situation. Sometimes a subject's arm is more stable and there is simply no arm motion to be captured. In general, the electrode location is highly sensitive for being able to obtain bioimpedance signal. If it is even a few centimeters off, the quality of signal obtained will be really low or even more, no signal will be obtained. Nonetheless, most of the data obtained, as mentioned, shows that the developed bioimpedance circuit is capable of obtaining both heart rate and respiration rate from the upper arm using bioimpedance.

6. SUMMARY

As it has been stated, there is a gap in the availability of wearable devices and sensors which are capable of measuring physiological values for different underrepresented populations. Because of that, the purpose of this research was to develop a system that utilizes bioimpedance techniques instead of light-based techniques. This system was made with the intention of obtaining important physiological values such as heart rate and respiration rate.

Looking at the values obtained and comparing between the developed PCB and the gold standard, it can be said that the system is successful in obtaining heart rate and respiration rate, which was the goal of the circuit. At times, respiration signal was not present in the PCB's signal, whereas in the Zephyr device it was present. It can be said that since the Zephyr uses a band wrapped around the lower chest area, it is easier to obtain respiration signal most of the times. However, the developed PCB system is better in terms of burden of use, since only an armband is needed, instead of a band that goes around your chest. Another issue one might notice is the sensitivity of the electrode location to obtain bioimpedance signal. In terms of the size, the developed circuit for testing had a small form factor which made it manageable to debug and test.

Some aspects of development of the circuit could be continued in future work. First, to solve the issue of finding an ideal electrode location, one can add a sensor, either analog or digital, that alerts the user when signal is not being collected. Then, it would allow him or her to readjust the armband until bioimpedance signal is being obtained correctly. Secondly, even though the developed circuit has a small form factor already, it can be made even smaller. Since the system uses basic components, they can be replaced by the use of

transistors. This would then make the circuit incredibly small which would allow it to be an ideal size for a wearable. Addition of these two solutions to the system will make it more robust, hopefully enabling it to be a feasible device for use in people who need to monitor their health.

REFERENCES

[1] Our World in Data. (2019). *Number of deaths by cause*. Our World in Data. Retrieved May 23, 2022, from https://ourworldindata.org/grapher/annual-number-of-deaths-by-cause

[2] Centers for Disease Control and Prevention. (2022, February 7). *Heart disease facts*. Centers for Disease Control and Prevention. Retrieved May 23, 2022, from https://www.cdc.gov/heartdisease/facts.htm

[3] Heidenreich, P. A., Trogdon, J. G., & Khavjou, O. A. (2011, January 24). *Forecasting the future of cardiovascular disease in the United States: A policy statement from the American Heart Association*. Circulation. Retrieved May 23, 2022, from https://pubmed.ncbi.nlm.nih.gov/21262990/

[4] Mouton, C. P. (2017, March). *Cardiovascular Health Disparities in underserved populations*. Primary care. Retrieved May 23, 2022, from https://pubmed.ncbi.nlm.nih.gov/28164826/

[5] *Vital signs (body temperature, pulse rate, respiration rate, blood pressure)*. Johns Hopkins Medicine. (n.d.). Retrieved February 15, 2022, from https://www.hopkinsmedicine.org/health/conditions-and-diseases/vital-signs-body-temperature-pulse-rate-respiration-rate-blood-pressure

[6] Bender, C. (2017, April 12). *Measuring the fitness of fitness trackers*. IEEE Xplore. Retrieved February 16, 2022, from https://ieeexplore.ieee.org/document/7894077

[7] Ghamari, M., Castaneda, D., & Esparza, A. (2018). A review on wearable photoplethysmography sensors and their potential future applications in health care. *International Journal of Biosensors & Bioelectronics*, *4*(4). https://doi.org/10.15406/ijbsbe.2018.04.00125

[8] Ahuja, N., Ozdalga, E., & Aaronson, A. (2016, July 8). *Integrating Mobile Fitness Trackers into the practice of medicine*. American journal of lifestyle medicine. Retrieved February 16, 2022, from https://www.ncbi.nlm.nih.gov/pmc/articles/PMC6124842/

[9] Food and Drug Administration. (n.d.). *De novo classification request for ECG app*. Access Data. Retrieved May 23, 2022, from https://www.accessdata.fda.gov/cdrh_docs/reviews/DEN180044.pdf

[10] A. Puranen, T. Halkola, O. Kirkeby and A. Vehkaoja, (2020) *Effect of skin tone and activity on the performance of wrist-worn optical beat-to-beat heart rate monitoring*. IEEE SENSORS, *1*(4). doi: 10.1109/SENSORS47125.2020.9278523.

[11] Boonya-Ananta, T., Rodriguez, A. J., Ajmal, A., Du Le, V. N., Hansen, A. K., Hutcheson, J. D., & Ramella-Roman, J. C. (2021, January 28). *Synthetic photoplethysmography (ppg) of the radial artery through parallelized Monte Carlo and its correlation to body mass index (BMI)*. Scientific reports. Retrieved May 23, 2022, from https://www.ncbi.nlm.nih.gov/pmc/articles/PMC7843978/

[12] Engmarksgaard, M. (2021, June). *Electrical impedance spectroscopy for use in oil quality assessment*. Retrieved April 11, 2022, from https://www.researchgate.net/publication/352329788_ELECTRICAL_IMPEDANCE_SPECTROSCOPY_FOR_USE_IN_OIL_QUALITY_ASSESSMENT

[13] Magar HS, Hassan RYA, Mulchandani A. Electrochemical Impedance Spectroscopy (EIS): Principles, Construction, and Biosensing Applications. *Sensors (Basel)*. 2021;21(19):6578. Published 2021 Oct 1. doi:10.3390/s21196578

[14] Earthman, C., Traughber, D., Dobratz, J., & Howell, W. (2007). Bioimpedance spectroscopy for clinical assessment of fluid distribution and body cell mass. *Nutrition in clinical practice : official publication of the American Society for Parenteral and Enteral Nutrition*, *22*(4), 389–405. https://doi.org/10.1177/0115426507022004389

[15] Kanoun, O. (2018, December 17). *Impedance spectroscopy*. De Gruyter. Retrieved February 19, 2022, from https://www.degruyter.com/document/doi/10.1515/9783110558920/html

[16] Earthman, C., Traughber D, D., & Howell, D. J. (n.d.). *Bioimpedance spectroscopy for clinical assessment of fluid distribution and body cell mass*. Nutrition in clinical practice : official publication of the American Society for Parenteral and Enteral Nutrition. Retrieved May 23, 2022, from https://pubmed.ncbi.nlm.nih.gov/17644693/

[17] Sel, K., Osman, D., & Jafari, R. (2021). *Non-invasive cardiac and respiratory activity assessment from various human body locations using bioimpedance*. IEEE open journal of engineering in medicine and biology. Retrieved May 23, 2022, from https://www.ncbi.nlm.nih.gov/pmc/articles/PMC8388562/

[18] Al-Harosh, M., Yangirov, M., Kolesnikov, D., & Shchukin, S. (2021, December 17). *Bio-impedance sensor for real-time artery diameter waveform assessment*. Sensors. Retrieved May 23, 2022, from https://www.ncbi.nlm.nih.gov/pmc/articles/PMC8709432/

[19] Al-Harosh, M., Kudashov, I., & Volkov, A. (2018, June 14). *The brachial artery localization for blood pressure monitoring using electrical impedance measurement*. IEEE

Xplore. Retrieved May 23, 2022, from https://ieeexplore.ieee.org/abstract/document/8384555/

[20] Grimnes1, S., & Martinsen1, Ø. G. (2010, April 1). *Alpha-dispersion in human tissue* IOPscience, Journal of Physics: Conference Series. Retrieved February 19, 2022, from https://iopscience.iop.org/article/10.1088/1742-6596/224/1/012073

[21] IEC 60601-1-11:2015 Medical electrical equipment — Part 1-11: General requirements for basic safety and essential performance — Collateral standard: Requirements for medical electrical equipment and medical electrical systems used in the home healthcare environment. ISO. (2020, September 9). Retrieved February 19, 2022, from https://www.iso.org/standard/65529.html

[22] Sherwood, A. (1990, January 27). *Methodological guidelines for impedance cardiography*. Psychophysiology. Retrieved February 20, 2022, from https://pubmed.ncbi.nlm.nih.gov/2187214/

[23] Yufera, A., & Rueda, A. (n.d.). *A method for bioimpedance measure with four- and two-electrode sensor systems*. IEEE Xplore. Retrieved May 23, 2022, from https://ieeexplore.ieee.org/document/4649662/

[24] Lamlih, A. (2018, November). *Design of an integrated bioimpedance measurement system for chronic* ... Research Gate. Retrieved May 23, 2022, from https://www.researchgate.net/publication/333385329_Design_of_an_Integrated_Bioimpedance_Measurement_System_for_Chronic_Monitoring_of_Biological_Tissue_Composition

[25] Kassanos, P., & Guang-Zhong, Y. (2015, October 19). *A tetrapolar bio-impedance sensing system for gastrointestinal tract monitoring*. IEEE Xplore. Retrieved May 23, 2022, from https://ieeexplore.ieee.org/document/7299403/

[26] Jeong, P., Lee, D., & Woo, E. (2010, April). *Wideband bio-impedance spectroscopy using voltage source and tetra ...* Research Gate. Retrieved May 23, 2022, from https://www.researchgate.net/publication/228999498_Wideband_bio-impedance_spectroscopy_using_voltage_source_and_tetra-polar_electrode_configuration

[27] Kassanos, P., & Guang-Zhong, Y. (2020, August 11). *A comparison of front-end amplifiers for tetrapolar bioimpedance measurements*. IEEE Xplore. Retrieved May 23, 2022, from https://ieeexplore.ieee.org/document/9164909/

[28] Chang, Z.-yao, Pop, G., & Meijer, G. (2008, April). *A comparison of two- and four-electrode techniques to Characterize Blood Impedance for the Frequency Range of 100 Hz to 100 MHz*. Retrieved February 21, 2022, from https://www.researchgate.net/publication/5518675_A_Comparison_of_Two-_and_Four-Electrode_Techniques_to_Characterize_Blood_Impedance_for_the_Frequency_Range_of_100_Hz_to_100_MHz

[29] Texas Instruments. (2015, June). *Opax277 High Precision Operational Amplifiers datasheet (rev. B)*. TI. Retrieved May 23, 2022, from https://www.ti.com/lit/ds/symlink/opa277.pdf

[30] SCrecraft, D. I., & Gergely, S. (2007, September 14). *Signal generation*. Analog Electronics. Retrieved May 23, 2022, from https://www.sciencedirect.com/science/article/pii/B9780750650953500118

[31] Texas Instruments. (2013, April). *An-1515 a comprehensive study of the Howland Current Pump (rev. A)*. TI. Retrieved May 23, 2022, from https://www.ti.com/lit/an/snoa474a/snoa474a.pdf

[32] Texas Instruments. (2018, January). *INA828 50-MV offset, 7-nv/√hz noise, low-power, precision ...* TI. Retrieved May 23, 2022, from https://www.ti.com/lit/ds/symlink/ina828.pdf

[33] National Instruments. (2016, October). *User guide NI mydaq*. NI. Retrieved May 23, 2022, from https://www.ni.com/pdf/manuals/373060g.pdf

[34] BIOPAC Systems, Inc. (n.d.). *MP160 starter systems: BIOPAC*. BIOPAC. Retrieved May 23, 2022, from https://www.biopac.com/product-category/research/systems/mp150-starter-systems/

[35] BIOPAC Systems, Inc. (n.d.). *Electrobioimpedance impedance cardiography (ICG) amplifier: EBI100C: Research: BIOPAC*. BIOPAC. Retrieved May 23, 2022, from https://www.biopac.com/product/electrobioimpedance-amplifier/

[36] Annus, P., & Lamp, J. (2005, October 31). *Design of a bioimpedance measurement system using direct carrier compensation*. IEEE Xplore. Retrieved May 23, 2022, from https://ieeexplore.ieee.org/document/1523051

[37] Science Direct. (n.d.). *Amplitude Modulation*. Sciencedirect. Retrieved May 23, 2022, from https://www.sciencedirect.com/topics/engineering/amplitude-modulation/pdf

[38] Texas Instruments. (2021, August). *OPAX191 Datasheet*. TI. Retrieved May 23, 2022, from https://www.ti.com/lit/ds/symlink/opa191.pdf

[39] Analog Devices. (n.d.). *Precision, dual-channel Instrumentation Amplifier Data Sheet AD8222*. Analog. Retrieved May 23, 2022, from https://www.analog.com/media/en/technical-documentation/data-sheets/AD8222.pdf

[40] Bseio, W., & Prasad, A. (2016, December 15). *Analysis of skin-electrode impedance using concentric ring electrode*. IEEE Xplore. Retrieved May 23, 2022, from https://ieeexplore.ieee.org/document/4463279

[41] Neuropsychology. (n.d.). *Neuropsychology/NeuroKit: Neurokit2: The python toolbox for Neurophysiological Signal Processing*. GitHub. Retrieved June 5, 2022, from https://github.com/neuropsychology/NeuroKit

APPENDIX A

BIOIMPEDANCE DATA COLLECTED FOR SUBJECT TWO USED FOR OBTAINING PHYSIOLOGICAL VALUES

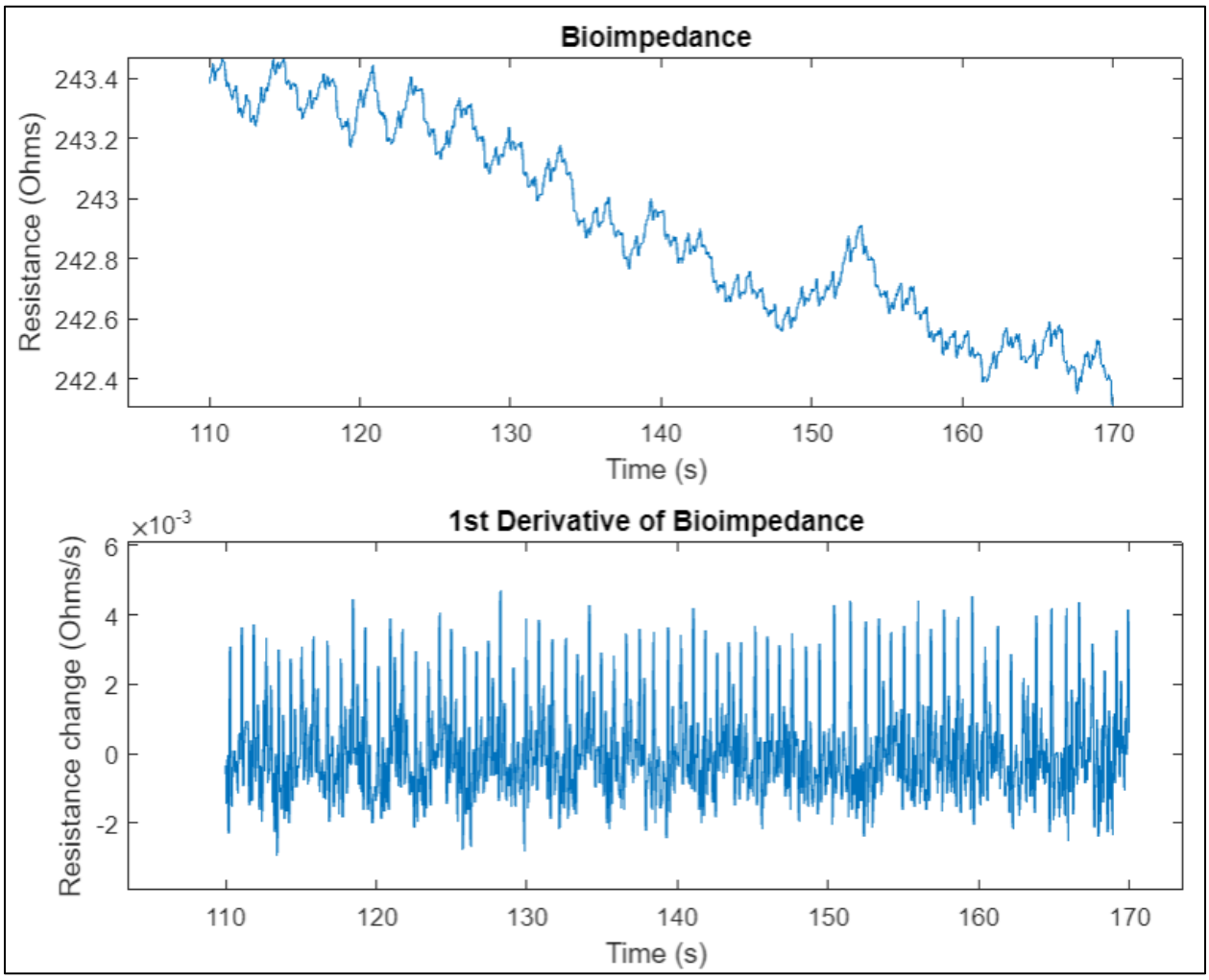

Figure A1. 60 seconds of bioimpedance signal collected

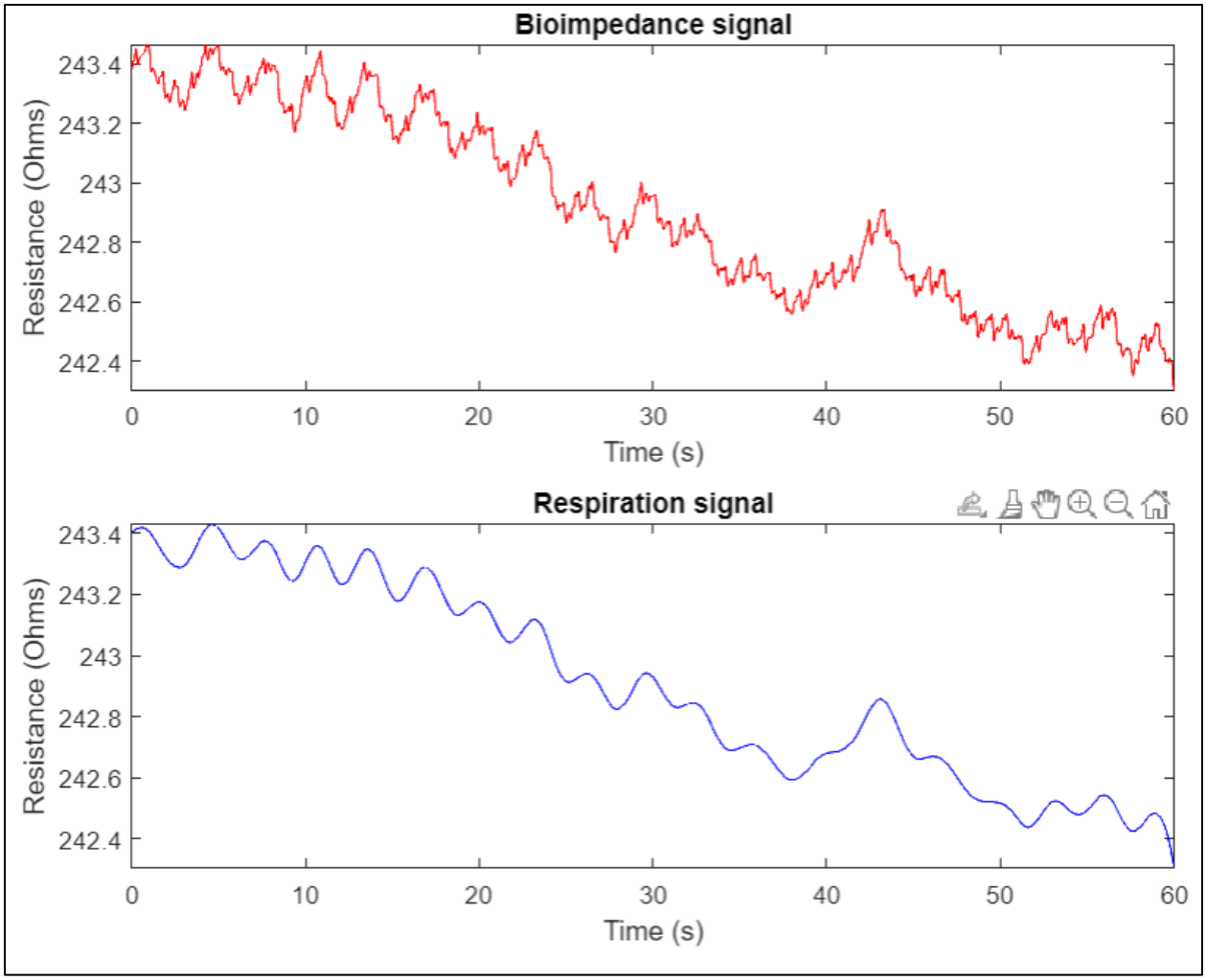

Figure A2. Respiration signal obtained from bioimpedance signal

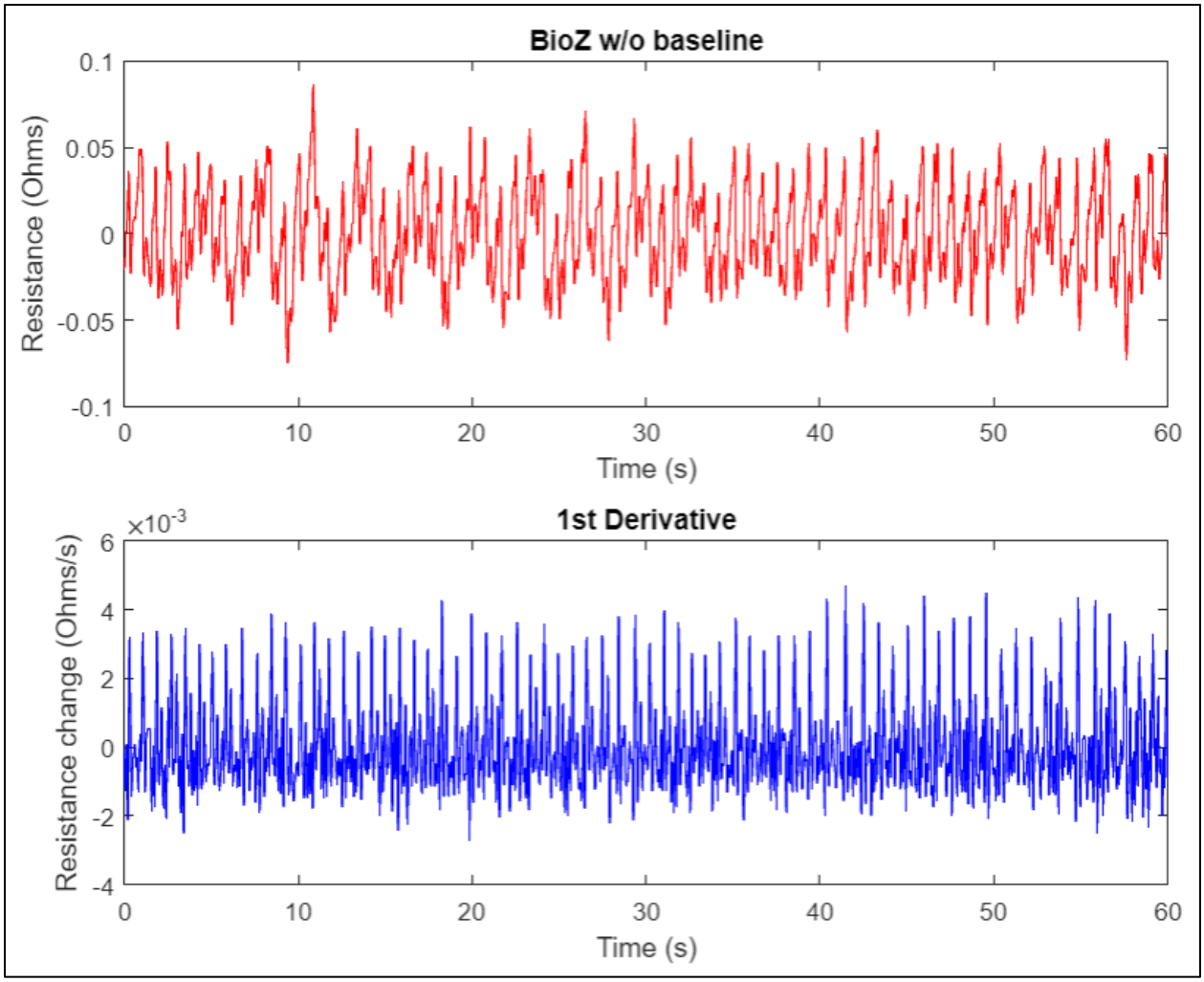

Figure A3. Bioimpedance signal and first derivative without low frequency components

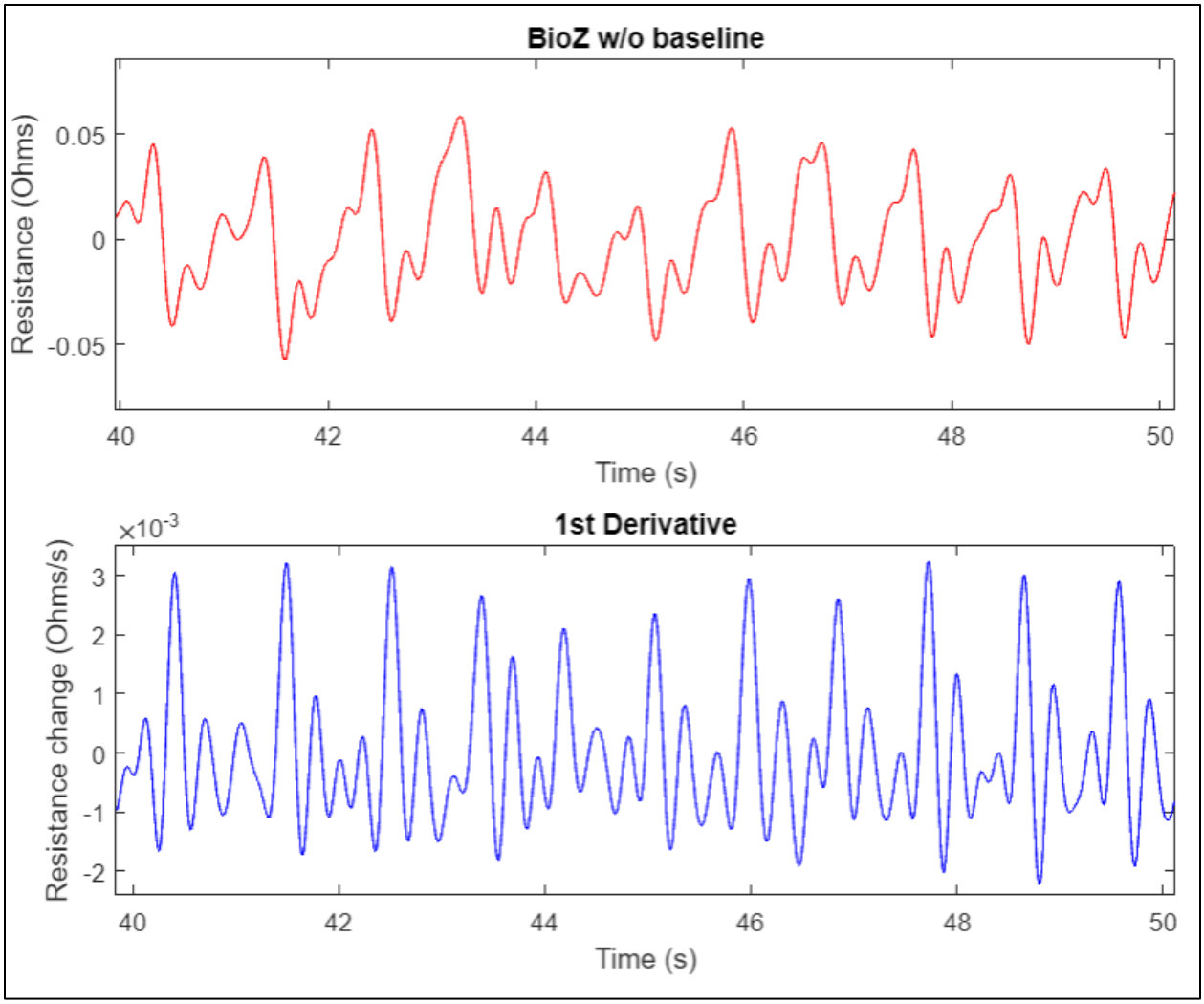

Figure A4. Bioimpedance signal and first derivative without low frequency components closeup

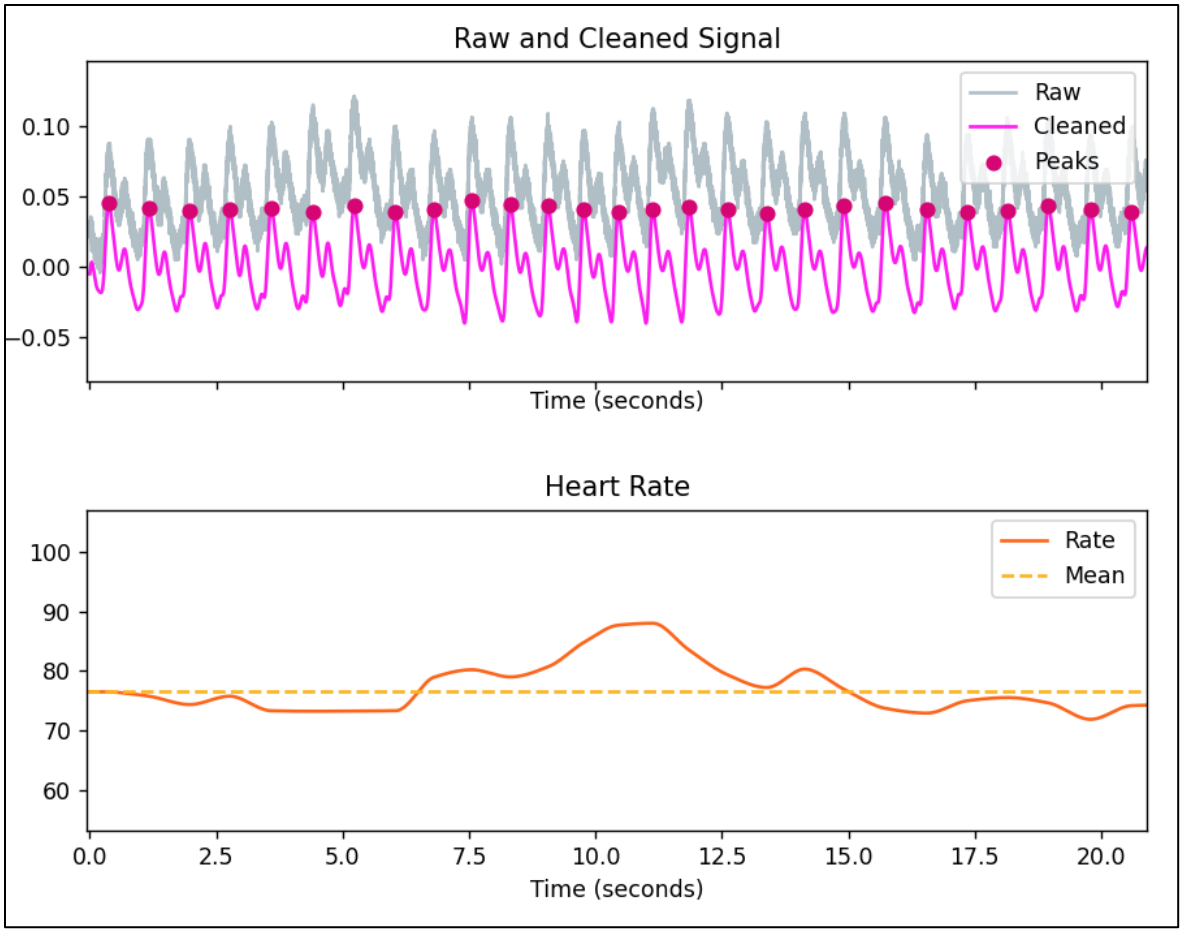

Figure A5. Peak detection for heart rate calculation

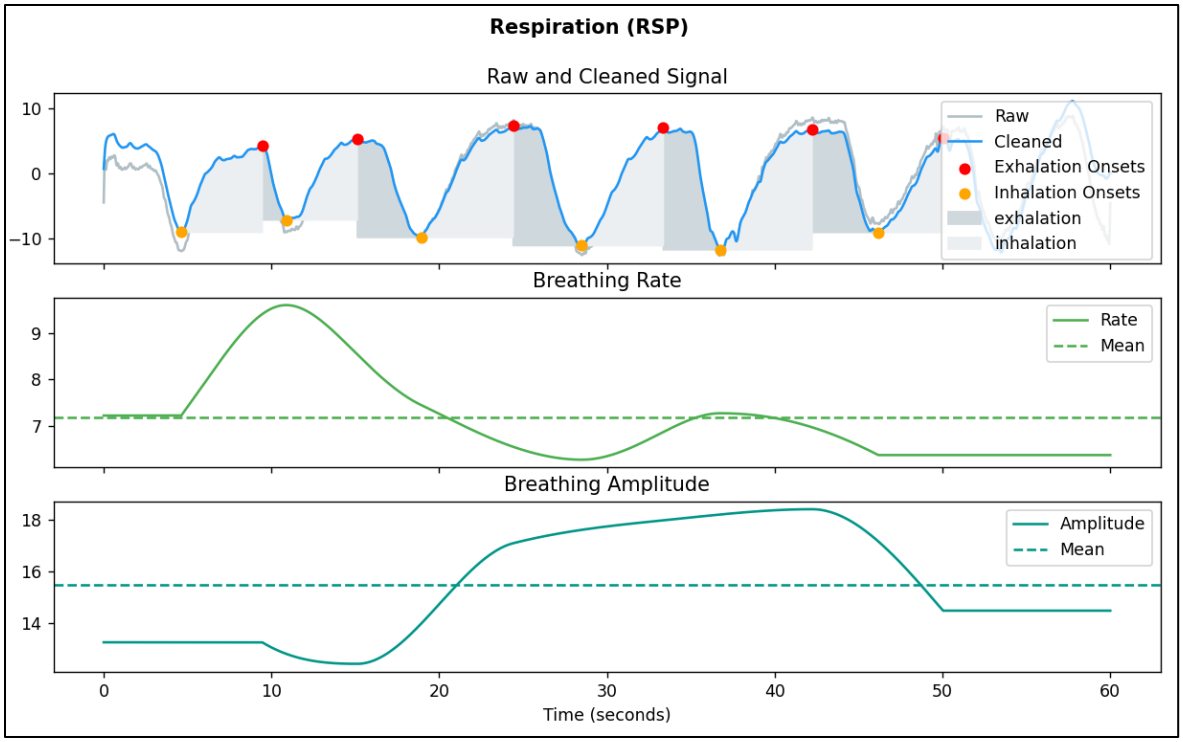

Figure A6. Peak detection for respiration rate calculation